

# Beta-CROWN: Efficient Bound Propagation with Per-neuron Split Constraints for Complete and Incomplete Neural Network Verification

Shiqi Wang<sup>\*,1</sup>      Huan Zhang<sup>\*,2,4</sup>      Kaidi Xu<sup>\*,3</sup>  
 Xue Lin<sup>3</sup>      Suman Jana<sup>1</sup>      Cho-Jui Hsieh<sup>2</sup>      J. Zico Kolter<sup>4</sup>

<sup>1</sup>Columbia University    <sup>2</sup>UCLA    <sup>3</sup>Northeastern University    <sup>4</sup>CMU

tcwangshiqi@cs.columbia.edu, huan@huan-zhang.com, xu.kaid@northeastern.edu  
 xue.lin@northeastern.edu, suman@cs.columbia.edu, chohsieh@cs.ucla.edu, zkoltter@cs.cmu.edu

<sup>\*</sup> Equal Contribution.

## Abstract

Recent works in neural network verification show that cheap incomplete verifiers such as CROWN, based upon bound propagations, can effectively be used in Branch-and-Bound (BaB) methods to accelerate complete verification, achieving significant speedups compared to expensive linear programming (LP) based techniques. However, they cannot fully handle the per-neuron split constraints introduced by BaB like LP verifiers do, leading to looser bounds and hurting their verification efficiency. In this work, we develop  $\beta$ -CROWN, a new bound propagation based method that can fully encode per-neuron splits via optimizable parameters  $\beta$ . When the optimizable parameters are jointly optimized in intermediate layers,  $\beta$ -CROWN has the potential of producing better bounds than typical LP verifiers with neuron split constraints, while being efficiently parallelizable on GPUs. Applied to the complete verification setting,  $\beta$ -CROWN is close to three orders of magnitude faster than LP-based BaB methods for robustness verification, and also over twice faster than state-of-the-art GPU-based complete verifiers with similar timeout rates. By terminating BaB early, our method can also be used for incomplete verification. Compared to the state-of-the-art semidefinite-programming (SDP) based verifier, we show a substantial leap forward by greatly reducing the *gap* between verified accuracy and empirical adversarial attack accuracy, from 35% (SDP) to 12% on an adversarially trained MNIST network ( $\epsilon = 0.3$ ), while being 47 times faster.

## 1. Introduction

As neural networks (NNs) begin to be deployed in safety-critical applications, it becomes increasingly important to formally verify their behaviors under potentially malicious

inputs. Broadly speaking, the neural network verification problem involves proving certain desired relationships between inputs and outputs (often referred to as *specifications*), such as safety or robustness guarantees, for all inputs inside some domain. Canonically, the problem can be cast as finding the global minima of some functions on the network’s outputs (e.g., the difference between the predictions of the true label and another target label), with a bounded input set as constraints. This is a challenging problem due to the non-convexity and high dimensionality of neural networks.

We first focus on complete verification: the verifier should give a definite “yes/no” answer given sufficient time. Many complete verifiers rely on the branch and bound (BaB) method (Bunel et al., 2018) involving (1) branching by recursively splitting the original verification problem into subdomains (e.g., splitting a ReLU neuron into positive/negative linear regions) and (2) bounding each subdomain with specialized incomplete verifiers. Traditional BaB-based verifiers use expensive linear programming (LP) solvers (Ehlers, 2017; Lu & Kumar, 2020; Bunel et al., 2020b) as incomplete verifiers which can fully encode neuron split constraints for tight bounding. Meanwhile, a recent work (Xu et al., 2021) shows that cheap incomplete verifiers can significantly accelerate complete verifiers on GPUs over LP-based ones thanks to their efficiency. We call these cheap incomplete verifiers *bound propagation methods* (Wong & Kolter, 2018; Dvijotham et al., 2018; Gehr et al., 2018; Singh et al., 2019b), i.e., maintaining and propagating tractable and sound bounds through the networks, and CROWN (Zhang et al., 2018) is a representative method in this category.

However, unlike LP solvers, existing bound propagation methods lack the power to handle neuron split constraints introduced by BaB. For instance, given  $x, y \in [-1, 1]$ , they can efficiently bound  $x+y$  as  $[-2, 2]$  but they have no means to consider neuron split constraints such as  $x - y \geq 1$  introduced by BaB. Such a problem causes loose bounds and unnecessary branching, hurting the verification efficiency. Even worse, they fail to detect many infeasible subdomains in BaB, leading to incompleteness unless additional check-

ing is performed (Xu et al., 2021).

In our work, we develop a new, fast bound propagation based incomplete verifier,  $\beta$ -CROWN. It solves an optimization problem equivalent to the expensive LP based methods with neuron split constraints while still enjoys the efficiency of bound propagation methods.  $\beta$ -CROWN contains optimizable parameters  $\alpha$  and  $\beta$ , and any valid settings of these parameters yield valid bounds. These parameters are optimized using a few steps of (super)gradient ascent to achieve bounds as tight as possible. Optimizing  $\beta$  can also eliminate many infeasible subdomains and avoid further useless branching. Furthermore, we can jointly optimize  $\alpha$  and  $\beta$  for intermediate layer bounds, allowing  $\beta$ -CROWN to tighten relaxations and outperform typical LP verifiers with fixed intermediate layer bounds. Unlike traditional LP-based BaB methods,  $\beta$ -CROWN can be efficiently implemented with an automatic differentiation framework on GPUs to fully exploit the power of modern machine learning accelerators. The combination of  $\beta$ -CROWN and BaB produces a complete verifier with GPU acceleration, reducing the verification time of traditional LP based BaB verifiers (Bunel et al., 2018) by almost *three orders of magnitudes* on standard benchmarking models. Compared to all state-of-the-art GPU-based complete verifiers (Bunel et al., 2020b; Xu et al., 2021; De Palma et al., 2021), our approach is 2 to 7 times faster with a similar timeout rates.

Finally, by terminating our complete BaB verifier with  $\beta$ -CROWN early, our approach can also function as a more accurate incomplete verifier by returning an incomplete but sound lower bound of all subdomains explored so far. Thanks to our efficiency and scalability, we are capable of verifying the  $\ell_\infty$  robustness of *verification-agnostic* networks within a short time. Our method substantially outperforms the existing state-of-the-art in incomplete verification, namely SDP-FO (Dathathri et al., 2020), based upon tight semidefinite programming (SDP) relaxations (Raghunathan et al., 2018; Dvijotham et al., 2020). For a 4-layer CNN network trained with traditional adversarial training on MNIST ( $\ell_\infty$  norm  $\epsilon = 0.3$ ), we improve the verified accuracy from 43% (SDP-FO) to 66%, getting much closer to empirical accuracy (78%) under PGD attacks. To achieve this level of verification, our solver only uses *3 minutes* for each verification instance while the state-of-the-art GPU-based SDP-FO takes *2 to 3 hours* per verification instance on the same GPU. In total, our approach represents a substantial leap forward in the accuracy and scalability of verification for verification-agnostic adversarially trained networks.

## 2. Background

### 2.1. The Neural Network Verification Problem

We define the input of a neural network as  $x \in \mathbb{R}^{d_0}$ , and define the weights and biases of an  $L$ -layer neural network

as  $\mathbf{W}^{(i)} \in \mathbb{R}^{d_i \times d_{i-1}}$  and  $\mathbf{b}^{(i)} \in \mathbb{R}^{d_i}$  ( $i \in \{1, \dots, L\}$ ) respectively. For simplicity we assume that  $d_L = 1$  so  $\mathbf{W}^{(L)}$  is a vector and  $\mathbf{b}^{(L)}$  is a scalar. The neural network function  $f : \mathbb{R}^{d_0} \rightarrow \mathbb{R}$  is defined as  $f(x) = z^{(L)}(x)$ , where  $z^{(i)}(x) = \mathbf{W}^{(i)}\hat{z}^{(i-1)}(x) + \mathbf{b}^{(i)}$ ,  $\hat{z}^{(i)}(x) = \sigma(z^{(i)}(x))$  and  $\hat{z}^{(0)}(x) = x$ .  $\sigma$  is the activation function and we use ReLU throughout this paper. When the context is clear, we omit  $\cdot(x)$  and use  $z_j^{(i)}$  and  $\hat{z}_j^{(i)}$  to represent the *pre-activation* and *post-activation* values of the  $j$ -th neuron in the  $i$ -th layer. Neural network verification seeks the solution of the following optimization problem:

$$\begin{aligned} \min f(x) &:= z^{(L)}(x) \\ \text{s.t. } z^{(i)} &= \mathbf{W}^{(i)}\hat{z}^{(i-1)} + \mathbf{b}^{(i)}, i \in \{1, \dots, L\} \\ \hat{z}^{(i)} &= \sigma(z^{(i)}), i \in \{1, \dots, L-1\} \\ x &\in \mathcal{C}. \end{aligned} \quad (1)$$

The set  $\mathcal{C}$  defines the allowed input region and our aim is to find the minimum of  $f(x)$  for  $x \in \mathcal{C}$ , and throughout this paper we consider  $\mathcal{C}$  as a  $\ell_\infty$  ball around a data example  $x_0$ :  $\mathcal{C} = \{x \mid \|x - x_0\|_\infty \leq \epsilon\}$ . In practical settings, we typically have “specifications” to verify, which are (usually linear) functions of neural network outputs describing the desired behavior of neural networks. For example, to guarantee robustness we typically investigate the margin between logits. Because the specification can also be seen as an output layer of NN and merged into  $f(x)$  under verification, we do not discuss it in detail in this work. We consider the canonical specification  $f(x) > 0$ : if we can prove that  $f(x) > 0, \forall x \in \mathcal{C}$ , we say  $f(x)$  is verified.

When  $\mathcal{C}$  is a convex set, Eq. 1 is still a non-convex problem because the constraints  $\hat{z}^{(i)} = \sigma(z^{(i)})$  are non-convex. Given unlimited time, *complete* verifiers can solve Eq. 1 exactly:  $f^* = \min f(x), \forall x \in \mathcal{C}$ , so we can always conclude if the specification holds or not for any problem instance. On the other hand, *incomplete* verifiers usually relax the non-convexity of neural networks to obtain a tractable lower bound of the solution  $\underline{f} \leq f^*$ . For cases where  $\underline{f} < 0$ , we cannot conclude if the specification is true or not.

A commonly used incomplete verifier is to relax non-convex ReLUs with linear constraints and turn the verification problem into a linear programming problem, which can then be solved with linear solvers. We refer to it as “LP verifier” in this paper. Specifically, given  $\text{ReLU}(z_j^{(i)}) := \max(0, z_j^{(i)})$  and its intermediate layer bounds  $1_j^{(i)} \leq z_j^{(i)} \leq \mathbf{u}_j^{(i)}$ , each ReLU can be categorized into three states linearly relaxed differently: (1) if  $1_j^{(i)} \geq 0$  (ReLU in linear region) then  $\hat{z}_j^{(i)} = z_j^{(i)}$ ; (2) if  $\mathbf{u}_j^{(i)} \leq 0$  (ReLU in inactive region) then  $\hat{z}_j^{(i)} = 0$ ; (3) if  $1_j^{(i)} \leq 0 \leq \mathbf{u}_j^{(i)}$  (ReLU is *unstable*) then three linear bounds are used:  $\hat{z}_j^{(i)} \geq 0$ ,  $\hat{z}_j^{(i)} \geq z_j^{(i)}$ , and  $\hat{z}_j^{(i)} \leq \frac{\mathbf{u}_j^{(i)}}{\mathbf{u}_j^{(i)} - 1_j^{(i)}} (z_j^{(i)} - 1_j^{(i)})$ . This popular

relaxation (Ehlers, 2017; Wong & Kolter, 2018) is often referred to as the “triangle” relaxation. The intermediate layer bounds  $\mathbf{l}^{(i)}$  and  $\mathbf{u}^{(i)}$  are usually obtained from a cheaper bound propagation method (see next subsection). LP verifiers can provide relatively tight bounds but linear solvers are usually expensive. Also, they have to use fixed intermediate bounds and cannot use the joint optimization of intermediate layer bound (Section 3.3) to tighten relaxation.

## 2.2. CROWN: Efficient Incomplete Verification by Propagating Linear Bounds

Another way to give a lower bound for the objective in Eq. 1 is through sound bound propagation. CROWN (Zhang et al., 2018) is a representative method that propagates a linear bound of  $f(x)$  w.r.t. every intermediate layer in a backward manner until reaching the input  $x$ . CROWN uses two linear constraints to relax unstable ReLU neurons: a linear upper bound  $\hat{z}_j^{(i)} \leq \frac{\mathbf{u}_j^{(i)}}{\mathbf{u}_j^{(i)} - \mathbf{l}_j^{(i)}} (z_j^{(i)} - \mathbf{l}_j^{(i)})$  and a linear lower bound  $\hat{z}_j^{(i)} \geq \alpha_j^{(i)} z_j^{(i)} (0 \leq \alpha_j^{(i)} \leq 1)$ . After employing the two bounds, we can bound the output of a ReLU layer:

**Lemma 2.1** (Relaxation of a ReLU layer in CROWN). *Given  $w, v \in \mathbb{R}^d$ ,  $\mathbf{u} \leq v \leq \mathbf{l}$  (element-wise), we have*

$$w^\top \text{ReLU}(v) \geq w^\top \mathbf{D}v + b',$$

where  $\mathbf{D}$  is a diagonal matrix containing free variables  $0 \leq \alpha_j \leq 1$  only when  $\mathbf{u}_j > 0 > \mathbf{l}_j$  and  $w_j \geq 0$ , while its rest values as well as constant  $b'$  are determined by  $\mathbf{l}, \mathbf{u}, w$ .

Detailed forms for each term can be found in Appendix A. Lemma 2.1 can be repeatedly applied to a multi-layer network, resulting in an efficient back-substitution procedure to derive a linear lower bound w.r.t.  $x$ :

**Lemma 2.2** (CROWN bound (Zhang et al., 2018)). *Given an  $L$ -layer ReLU NN  $f(x) : \mathbb{R}^{d_0} \rightarrow \mathbb{R}$  with weights  $\mathbf{W}^{(i)}$ , biases  $\mathbf{b}^{(i)}$ , pre-ReLU bounds  $\mathbf{l}^{(i)} \leq z^{(i)} \leq \mathbf{u}^{(i)}$  ( $1 \leq i \leq L$ ) and input constraint  $x \in \mathcal{C}$ . We have*

$$\min_{x \in \mathcal{C}} f(x) \geq \min_{x \in \mathcal{C}} \mathbf{a}_{\text{CROWN}}^\top x + c_{\text{CROWN}}$$

where  $\mathbf{a}_{\text{CROWN}}$  and  $c_{\text{CROWN}}$  can be computed using  $\mathbf{W}^{(i)}, \mathbf{b}^{(i)}, \mathbf{l}^{(i)}, \mathbf{u}^{(i)}$  in polynomial time.

When  $\mathcal{C}$  is an  $\ell_p$  norm ball, minimization over the linear function can be easily solved using Hölder’s inequality. The main benefit of CROWN is its efficiency: CROWN can be efficiently implemented on machine learning accelerators such as GPUs (Xu et al., 2020) and TPUs (Zhang et al., 2020), and it can be a few magnitudes faster than an LP verifier which is hard to parallelize on GPUs. CROWN has been generalized to general network architectures (Xu et al., 2020; Shi et al., 2020) while we only demonstrate it for feedforward ReLU networks for simplicity.

## 2.3. Branch and Bound and Neuron Split Constraints

Complete neural network verifiers must solve Eq. 1 exactly rather than giving a lower bound. In ReLU networks, because ReLU is piece-wise linear, we can split each unstable neuron  $z_j^{(i)}$  into two cases:  $z_j^{(i)} \geq 0$  and  $z_j^{(i)} < 0$ . If there are  $N$  unstable neurons, a total of  $2^N$  cases will be produced and in each case the constraints  $\hat{z}^{(i)} = \sigma(z^{(i)})$  become linear constraints and can be solved exactly via linear programming. A smarter way to handle problems with this structure is branch and bound (BaB) (Bunel et al., 2018): we divide the domain of the verification problem  $\mathcal{C}$  into two subdomains  $\mathcal{C}_1 = \{x \in \mathcal{C}, z_j^{(i)} \geq 0\}$  and  $\mathcal{C}_2 = \{x \in \mathcal{C}, z_j^{(i)} < 0\}$  where  $z_j^{(i)}$  is an unstable neuron. Both subproblems can be solved using incomplete verifiers with relaxations. If the lower bound produced for subdomain  $\mathcal{C}_i$  (denoted by  $f_{\mathcal{C}_i}$ ) is greater than 0,  $\mathcal{C}_i$  is verified; otherwise, we further branch over domain  $\mathcal{C}_i$  by splitting another unstable ReLU neuron. The process terminates when all subdomains are verified.

A popular incomplete verifier used in BaB is the LP verifier. Essentially, when we split the  $j$ -th ReLU in layer  $i$ , we can simply add  $z_j^{(i)} \geq 0$  or  $z_j^{(i)} < 0$  to Eq. 1, relax both problems using linear relaxation, and solve them. We denote the  $\mathcal{Z}^{+(i)}$  as the set of neuron indices with positive split constraints and  $\mathcal{Z}^{-(i)}$  for neuron indices with negative split constraints in layer  $i$ . We define the split constraints at layer  $i$  as  $\mathcal{Z}^{(i)} := \{z^{(i)} \mid z_{j_1}^{(i)} \geq 0, z_{j_2}^{(i)} < 0, \forall j_1 \in \mathcal{Z}^{+(i)}, \forall j_2 \in \mathcal{Z}^{-(i)}\}$ . We denote the vector of all pre-ReLU neurons as  $z$ , and we define a set  $\mathcal{Z}$  to represent the split constraints on  $z$ :  $\mathcal{Z} = \mathcal{Z}^{(1)} \cap \mathcal{Z}^{(2)} \cap \dots \cap \mathcal{Z}^{(L-1)}$ . For convenience, we also use the shorthand  $\tilde{\mathcal{Z}}^{(i)} := \mathcal{Z}^{(1)} \cap \dots \cap \mathcal{Z}^{(i)}$  and  $\tilde{z}^{(i)} := \{z^{(1)}, z^{(2)}, \dots, z^{(i)}\}$ . These constraints can be easily handled by LPs, however LPs are typically significantly expensive than cheap bound propagation methods such as CROWN and cannot be easily accelerated on GPUs.

## 3. $\beta$ -CROWN for Complete and Incomplete Verification

In this section, we first give intuitions on handling split constraints during a bound propagation process. Then we formally state the main theorem of  $\beta$ -CROWN bounds from both primal space and dual space, and discuss how to tighten the bound using free parameters  $\alpha$  and  $\beta$ . Lastly, we propose  $\beta$ -CROWN BaBSR, a complete verifier that also becomes a strong incomplete verifier when stopped early.

### 3.1. $\beta$ -CROWN: Linear Bound Propagation with Neuron Split Constraints

The verification problem under split constraints can be written as an optimization problem:

$$\min_{x \in \mathcal{C}, z \in \mathcal{Z}} f(x).$$

Existing bound propagation algorithm such as CROWN can give a relatively tight lower bound for  $\min_{x \in \mathcal{C}} f(x)$  via efficient linear bound propagation but they *cannot handle the split constraints*  $z \in \mathcal{Z}$ . Before we present our main theorem, we first show the intuition on how to apply split constraints to the bound propagation process.

To encode the neuron splits, we first define diagonal matrix  $\mathbf{S}^{(i)} \in \mathbb{R}^{d_i \times d_i}$ ,  $i \in [1, \dots, L-1]$  where

$$\mathbf{S}_{j,j}^{(i)} = \begin{cases} -1, & \text{if we split } z_j^{(i)} \geq 0 \\ +1, & \text{if we split } z_j^{(i)} < 0 \\ 0, & \text{if we do not split } z_j^{(i)} \end{cases}, \quad j \in [1, \dots, d_i].$$

We start from the last layer, and derive linear bounds for each intermediate layer  $z^{(i)}$  and  $\hat{z}^{(i)}$  for both  $x \in \mathcal{C}$  and  $z \in \mathcal{Z}$ . We also assume that pre-ReLU bounds  $\mathbf{l}^{(i)} \leq z^{(i)} \leq \mathbf{u}^{(i)}$  for each layer  $i$  are available. We initially have:

$$\min_{x \in \mathcal{C}, z \in \mathcal{Z}} f(x) = \min_{x \in \mathcal{C}, z \in \mathcal{Z}} \mathbf{W}^{(L)} \hat{z}^{(L-1)} + \mathbf{b}^{(L)}. \quad (2)$$

Since  $\hat{z}^{(L-1)} = \text{ReLU}(z^{(L-1)})$ , we can apply Lemma 2.1 to relax the ReLU neuron at layer  $L-1$ , and obtain a linear lower bound for  $f(x)$  w.r.t.  $z^{(L-1)}$ :

$$\min_{x \in \mathcal{C}, z \in \mathcal{Z}} f(x) \geq \min_{x \in \mathcal{C}, z \in \mathcal{Z}} \mathbf{W}^{(L)} \mathbf{D}^{(L-1)} z^{(L-1)} + \text{const}.$$

To enforce the split neurons at layer  $L-1$ , we use a Lagrange function with  $\beta^{(L-1)\top} \mathbf{S}^{(L-1)}$  multiplied on  $z^{(L-1)}$ :

$$\begin{aligned} \min_{x \in \mathcal{C}, z \in \mathcal{Z}} f(x) &\geq \min_{\substack{x \in \mathcal{C} \\ z^{(L-2)} \in \hat{\mathcal{Z}}^{(L-2)}}} \max_{\beta^{(L-1)} \geq 0} \mathbf{W}^{(L)} \mathbf{D}^{(L-1)} z^{(L-1)} \\ &\quad + \beta^{(L-1)\top} \mathbf{S}^{(L-1)} z^{(L-1)} + \text{const} \\ &\geq \max_{\beta^{(L-1)} \geq 0} \min_{\substack{x \in \mathcal{C} \\ z^{(L-2)} \in \hat{\mathcal{Z}}^{(L-2)}}} \left( \mathbf{W}^{(L)} \mathbf{D}^{(L-1)} \right. \\ &\quad \left. + \beta^{(L-1)\top} \mathbf{S}^{(L-1)} \right) z^{(L-1)} + \text{const} \end{aligned} \quad (3)$$

The first inequality is due to the definition of the Lagrange function: we remove the constraint  $z^{(L-1)} \in \mathcal{Z}^{(L-1)}$  and use a multiplier to replace this constraint. The second inequality is due to weak duality. Due to the design of  $\mathbf{S}^{(L-1)}$ , neuron split  $z_j^{(L-1)} \geq 0$  has a negative multiplier  $-\beta_j^{(L-1)}$  and neuron split  $z_j^{(L-1)} < 0$  has a positive multiplier  $\beta_j^{(L-1)}$ . Any  $\beta^{(L-1)} \geq 0$  yields a lower bound for the constrained optimization problem. Then, for the next layer we substitute  $z^{(L-1)}$  with  $\mathbf{W}^{(L-1)} \hat{z}^{(L-2)} + \mathbf{b}^{(L-1)}$ :

$$\begin{aligned} \min_{x \in \mathcal{C}, z \in \mathcal{Z}} f(x) &\geq \max_{\beta^{(L-1)} \geq 0} \min_{\substack{x \in \mathcal{C} \\ z^{(L-2)} \in \hat{\mathcal{Z}}^{(L-2)}}} \left( \mathbf{W}^{(L)} \mathbf{D}^{(L-1)} \right. \\ &\quad \left. + \beta^{(L-1)\top} \mathbf{S}^{(L-1)} \right) \mathbf{W}^{(L-1)} \hat{z}^{(L-2)} + \text{const} \end{aligned} \quad (4)$$

We define a matrix  $\mathbf{A}^{(i)}$  to represent the linear relationship between  $f(x)$  and  $\hat{z}^{(i)}$ , where  $\mathbf{A}^{(L-1)} = \mathbf{W}^{(L)}$

according to Eq. 2 and  $\mathbf{A}^{(L-2)} = (\mathbf{A}^{(L-1)} \mathbf{D}^{(L-1)} + \beta^{(L-1)\top} \mathbf{S}^{(L-1)}) \mathbf{W}^{(L-1)}$  by Eq. 4. Since we consider  $f(x)$  with 1 dimensional output, essentially  $\mathbf{A}^{(i)}$  has only 1 row. After defining  $\mathbf{A}^{(L-2)}$ , we can rewrite Eq. 4 as:

$$\min_{x \in \mathcal{C}, z \in \mathcal{Z}} f(x) \geq \max_{\substack{\beta^{(L-1)} \geq 0 \\ z \in \mathcal{Z}}} \min_{\substack{x \in \mathcal{C} \\ z^{(L-2)} \in \hat{\mathcal{Z}}^{(L-2)}}} \mathbf{A}^{(L-2)} \hat{z}^{(L-2)} + \text{const},$$

which is in a form similar to Eq. 2 except for the outer maximization over  $\beta^{(L-1)}$ . This allows the back-substitution process (Eq. 2, Eq. 3, and Eq. 4) to continue. In each step, we swap max and min as in Eq. 3, so every maximization over  $\beta^{(i)}$  is outside of  $\min_{x \in \mathcal{C}}$ . Eventually, we have:

$$\min_{x \in \mathcal{C}, z \in \mathcal{Z}} f(x) \geq \max_{\beta \geq 0} \min_{x \in \mathcal{C}} \mathbf{A}^{(0)} x + \text{const},$$

where  $\beta := [\beta^{(1)\top} \beta^{(2)\top} \dots \beta^{(L-1)\top}]^\top$  concatenates all  $\beta^{(i)}$  vectors. Following the above idea, we present the main theorem in Theorem 3.1 (proof is given Appendix A).

**Theorem 3.1** ( $\beta$ -CROWN bound). *Given an  $L$ -layer neural network  $f(x) : \mathbb{R}^{d_0} \rightarrow \mathbb{R}$  with weights  $\mathbf{W}^{(i)}$ , biases  $\mathbf{b}^{(i)}$ , pre-ReLU bounds  $\mathbf{l}^{(i)} \leq z^{(i)} \leq \mathbf{u}^{(i)}$  ( $1 \leq i \leq L$ ), input constraint  $\mathcal{C}$  and split constraints  $\mathcal{Z}$ . We have*

$$\min_{x \in \mathcal{C}, z \in \mathcal{Z}} f(x) \geq \max_{\beta \geq 0} \min_{x \in \mathcal{C}} (\mathbf{a} + \mathbf{P}\beta)^\top x + \mathbf{q}^\top \beta + c, \quad (5)$$

where  $\mathbf{P} \in \mathbb{R}^{d_0 \times (\sum_{i=1}^{L-1} d_i)}$ ,  $\mathbf{q} \in \mathbb{R}^{\sum_{i=1}^{L-1} d_i}$ ,  $c$  is a constant.  $\mathbf{a}$ ,  $\mathbf{P}$ ,  $\mathbf{q}$  and  $c$  are functions of  $\mathbf{W}^{(i)}$ ,  $\mathbf{b}^{(i)}$ ,  $\mathbf{l}^{(i)}$  and  $\mathbf{u}^{(i)}$ .

Detailed formulations for  $\mathbf{a}$ ,  $\mathbf{P}$ ,  $\mathbf{q}$  and  $c$  are given in Appendix A. Theorem 3.1 shows that when neuron split constraints exist,  $f(x)$  can still be bounded by a linear equation containing optimizable multipliers  $\beta$ . Observing Eq. 3, the main difference between CROWN and  $\beta$ -CROWN during the bound propagation procedure lies in the relaxation of the ReLU layer, where we need an extra term  $\beta^{(i)\top} \mathbf{S}^{(i)}$  in the linear relationship matrix (for example,  $\mathbf{W}^{(L)} \mathbf{D}^{(L-1)}$  in Eq. 3) between  $f(x)$  and  $z^{(i)}$  to enforce neuron split constraints. This extra term in every ReLU layer yields  $\mathbf{P}$  and  $\mathbf{q}$  in Eq. 5 after bound propagation.

To solve the optimization problem in Eq. 5, we note that in the  $\ell_p$  norm robustness setting ( $\mathcal{C} = \{x \mid \|x - x_0\|_p \leq \epsilon\}$ ), the inner minimization has a closed solution:

$$\begin{aligned} \min_{x \in \mathcal{C}, z \in \mathcal{Z}} f(x) &\geq \max_{\substack{\beta \geq 0 \\ z \in \mathcal{Z}}} -\|\mathbf{a} + \mathbf{P}\beta\|_q \epsilon + (\mathbf{P}^\top x_0 + \mathbf{q})^\top \beta \\ &\quad + \mathbf{a}^\top x_0 + c := \max_{\beta \geq 0} g(\beta) \end{aligned} \quad (6)$$

where  $\frac{1}{p} + \frac{1}{q} = 1$ . The maximization is concave in  $\beta$  ( $q \geq 1$ ), so we can simply optimize it using projected (super)gradient ascent with gradients from an automatic differentiation library. Since any  $\beta \geq 0$  yields a valid lower bound for  $\min_{x \in \mathcal{C}, z \in \mathcal{Z}} f(x)$ , convergence is not necessary to guarantee soundness.  $\beta$ -CROWN is efficient - it has the same

asymptotic complexity as CROWN when  $\beta$  is fixed. When  $\beta = 0$ ,  $\beta$ -CROWN yields the same results as CROWN; however the additional optimizable  $\beta$  allows us to maximize and tighten the lower bound due to neuron split constraints.

In Lemma 2.1 we show that a free variable is associated with some unstable ReLU neurons. We define  $\alpha^{(i)} \in \mathbb{R}^{d_i}$  as a vector representing free variables for layer  $i$ . If a ReLU neuron  $j'$  at layer  $i$  does not contain this free variable (e.g., if the neuron is always 0 because  $\mathbf{u}_{j'}^{(i)} < 0$ ) we can simply ignore  $\alpha_{j'}^{(i)}$ . We define  $\alpha = \{\alpha^{(1)} \dots \alpha^{(L-1)}\}$  containing all free variables. Since any  $0 \leq \alpha_j^{(i)} \leq 1$  yields a valid bound, we can optimize this variable to tighten the bound. Formally, we rewrite Eq. 6 with  $\alpha$  explicitly:

$$\min_{x \in \mathcal{C}, z \in \mathcal{Z}} f(x) \geq \max_{0 \leq \alpha \leq 1, \beta \geq 0} g(\alpha, \beta). \quad (7)$$

### 3.2. Connection to the Dual Problem

In this subsection, we show that  $\beta$ -CROWN can also be derived from a dual LP problem. Based on Eq. 1 and linear relaxations in Section 2.1, we first construct an LP problem for  $\ell_\infty$  robustness verification with neuron split constraints:

$$\begin{aligned} \min f(x) &:= z^{(L)}(x) \\ \text{s.t. } z^{(i)} &= \mathbf{W}^{(i)} \hat{z}^{(i-1)} + \mathbf{b}^{(i)}, i \in \{1, \dots, L\} \\ \hat{z}^{(i)} &= z^{(i)}, i \in \{1, \dots, L-1\}, \mathbf{l}_j^{(i)} \geq 0 \text{ or } j \in \mathcal{Z}^{+(i)} \\ \hat{z}^{(i)} &= 0, i \in \{1, \dots, L-1\}, \mathbf{u}_j^{(i)} \leq 0 \text{ or } j \in \mathcal{Z}^{-(i)} \\ \hat{z}_j^{(i)} &\geq 0 \\ \hat{z}_j^{(i)} &\geq z_j^{(i)} \\ \hat{z}_j^{(i)} &\leq \frac{\mathbf{u}_j^{(i)}}{\mathbf{u}_j^{(i)} - \mathbf{l}_j^{(i)}} \left( z_j^{(i)} - \mathbf{l}_j^{(i)} \right) \end{aligned} \quad \left\{ \begin{array}{l} i \in \{1, \dots, L-1\} \\ \mathbf{l}_j^{(i)} < 0 < \mathbf{u}_j^{(i)} \\ j \notin \mathcal{Z}^{+(i)} \text{ and } j \notin \mathcal{Z}^{-(i)} \end{array} \right. \quad (8)$$

$$\begin{aligned} z_j^{(i)} &\geq 0, i \in \{1, \dots, L-1\}, j \in \mathcal{Z}^{+(i)} \\ z_j^{(i)} &< 0, i \in \{1, \dots, L-1\}, j \in \mathcal{Z}^{-(i)} \\ \hat{z}^{(0)} &\geq x_0 - \epsilon \\ \hat{z}^{(0)} &\leq x_0 + \epsilon \end{aligned}$$

Compared to the formulation in Wong & Kolter (2018), we have neuron split constraints  $\hat{z}_j^{(i)} \geq 0$  and  $\hat{z}_j^{(i)} < 0$  for  $j \in \mathcal{Z}^{+(i)}$  and  $j \in \mathcal{Z}^{-(i)}$  in Eq. 8. Many BaB based complete verifiers (Bunel et al., 2018; Lu & Kumar, 2020) use an LP solver for Eq. 8 as the incomplete verifier. We first show that it is possible to derive Theorem 3.1 from the dual of this LP, leading to Theorem 3.2:

**Theorem 3.2.** *The objective  $d_{LP}$  for the dual problem of Eq. 8 can be represented as*

$$d_{LP} = -\|\mathbf{a} + \mathbf{P}\beta\|_1 \cdot \epsilon + (\mathbf{P}^\top x_0 + \mathbf{q})^\top \beta + \mathbf{a}^\top x_0 + c,$$

where  $\mathbf{a}$ ,  $\mathbf{P}$ ,  $\mathbf{q}$  and  $c$  are defined in the same way as in Theorem 3.1, and  $\beta \geq 0$  corresponds to the dual variables of neuron split constraints in Eq. 8.

A similar connection between CROWN and dual LP based verifier (Wong & Kolter, 2018) was shown in (Salman et al., 2019), and their results can be seen as a special case of ours when  $\beta = 0$  and none of the split constraints are active. An immediate consequence is that  $\beta$ -CROWN can potentially give solutions as good as solving Eq. 8 using an LP solver:

**Corollary 3.2.1.** *When  $\alpha$  and  $\beta$  are optimally set,  $\beta$ -CROWN produces the same solution as LP with split constraints when intermediate bounds  $\mathbf{l}, \mathbf{u}$  are fixed. Formally,*

$$\max_{0 \leq \alpha \leq 1, \beta \geq 0} g(\alpha, \beta) = p_{LP}^*,$$

where  $p_{LP}^*$  is the optimal objective of Eq. 8.

In Appendix A we give detailed formulations for conversions between the variables  $\alpha, \beta$  in  $\beta$ -CROWN and their corresponding dual variables in the LP problem.

### 3.3. Joint optimization of free variables in $\beta$ -CROWN

In Eq. 7,  $g$  is also a function of  $\mathbf{l}_j^{(i)}$  and  $\mathbf{u}_j^{(i)}$ , the intermediate layer bounds for each neuron  $z_j^{(i)}$ .  $\mathbf{l}_j^{(i)}$  and  $\mathbf{u}_j^{(i)}$  are also computed using  $\beta$ -CROWN. For example, to obtain  $\mathbf{l}_j^{(i)}$ , we set  $f(x) := z_j^{(i)}(x)$  and apply Theorem 3.1:

$$\min_{x \in \mathcal{C}, \hat{z}^{(i-1)} \in \tilde{\mathcal{Z}}^{(i-1)}} z_j^{(i)}(x) \geq \max_{0 \leq \alpha' \leq 1, \beta' \geq 0} g'(\alpha', \beta') := \mathbf{l}_j^{(i)} \quad (9)$$

and for  $\mathbf{u}_j^{(i)}$  we set  $f(x) := -z_j^{(i)}(x)$ . Importantly, during solving these intermediate layer bounds, the  $\alpha'$  and  $\beta'$  are *independent sets of variables*, not the same ones for the objective  $f(x) := z^{(L)}$ . Since  $g$  is a function of  $\mathbf{l}_j^{(i)}$ , it is also a function of  $\alpha'$  and  $\beta'$ . In fact, there are a total of  $\sum_{i=1}^{L-1} d_i$  intermediate layer neurons, and each neuron is associated with a set of independent  $\alpha'$  and  $\beta'$  variables. Optimizing these variables allowing us to tighten the relaxations on unstable ReLU neurons (which depend on  $\mathbf{l}_j^{(i)}$  and  $\mathbf{u}_j^{(i)}$ ) and produce tight final bounds, which is impossible in LP. In other words, we need to optimize  $\hat{\alpha}$  and  $\hat{\beta}$ , which are two vectors concatenating  $\alpha$ ,  $\beta$  as well as a large number of  $\alpha'$  and  $\beta'$  used to compute each intermediate layer bound:

$$\min_{x \in \mathcal{C}, z \in \mathcal{Z}} f(x) \geq \max_{0 \leq \hat{\alpha} \leq 1, \hat{\beta} \geq 0} g(\hat{\alpha}, \hat{\beta}). \quad (10)$$

This formulation is non-convex and has a large number of variables. Since any  $0 \leq \hat{\alpha} \leq 1, \hat{\beta} \geq 0$  leads to a valid lower bound, the non-convexity does not affect soundness, and when intermediate layer bounds are also allowed to be tightened during optimization, we can outperform the LP problem Eq. 8 with fixed intermediate layer bounds. Typically, when Eq. 8 is formed, a bound propagation procedure is used to pre-compute intermediate layer bounds (Bunel et al., 2018; Lu & Kumar, 2020), which are far from optimal.

To estimate the dimension of this problem, we denote the number of unstable neurons at layer  $i$  as  $s_i := \text{Tr}(|\mathbf{S}^{(i)}|)$ . Each neuron in layer  $i$  is associated with  $2 \times \sum_{k=1}^{i-1} s_i$  variables  $\alpha'$ . Suppose each hidden layer has the same number of  $d$  neurons and  $s_i = O(d)$ , then the total number of variables in  $\alpha$  is  $2 \times \sum_{i=1}^{L-1} d_i \sum_{k=1}^{i-1} s_i = O(L^2 d^2)$ . This can be too large for efficient optimization, so we share  $\alpha'$  and  $\beta'$  among the intermediate neurons of the same layer, leading to a total number of  $O(L^2 d)$  variables to optimize.

### 3.4. $\beta$ -CROWN with Branch and Bound

We perform complete verification following the branch and bound (BaB) framework (Bunel et al., 2018) with  $\beta$ -CROWN as the incomplete solver, and we use the simple BaBSR branching heuristic (Bunel et al., 2020b). To efficiently utilize GPU, we also use batch splits to evaluate multiple subdomains in the same batch as in (Xu et al., 2020; De Palma et al., 2021). We list our full complete verification algorithm,  $\beta$ -CROWN BaBSR in Appendix B. We show that  $\beta$ -CROWN with BaB is complete:

**Theorem 3.3.**  *$\beta$ -CROWN with Branch and Bound on Splitting ReLU neurons (BaBSR) is sound and complete.*

Soundness is trivial because  $\beta$ -CROWN is a sound verifier. For completeness, it suffices to show that when all unstable ReLU neurons are split,  $\beta$ -CROWN gives the global minimum for Eq. 8. In contrast, combining CROWN (Zhang et al., 2018) with BaB does *not* yield a complete verifier, as it cannot detect infeasible splits and a slow LP solver is still needed to guarantee completeness (Xu et al., 2021). Instead,  $\beta$ -CROWN can detect infeasible subdomains - according to duality theory, an infeasible primal problem leads to an unbounded dual objective, which can be detected.

Additionally, we show the potential of *early stopping a complete verifier as an incomplete verifier*. BaB approaches the exact solution of Eq. 1 by splitting the problem into multiple subdomains, and more subdomains give a tighter lower bound for Eq. 1. Unlike traditional complete verifiers,  $\beta$ -CROWN is so efficient and can explore a large number of subdomains during a very short time, leading to huge improvements on the lower bounds and making BaB an attractive solution for efficient incomplete verification. In Section 4.1 we will show that  $\beta$ -CROWN with BaB can outperform a strong semidefinite-programming based incomplete solver with 60x speedup on average.

The success of  $\beta$ -CROWN comes from a few factors. First, in Section 3.1, we show that  $\beta$ -CROWN is an GPU-friendly bound propagation algorithm *significantly faster than LP solvers*. Second, in Section 3.2, we show that  $\beta$ -CROWN is solving an equivalent problem of the LP verifier *with neuron split constraints*. Third, in Section 3.3 we show that by jointly optimizing intermediate layer bounds,  $\beta$ -CROWN

can tighten relaxations and *achieve tighter bounds than typical LP verifiers* with fixed intermediate layer bounds.

## 4. Experimental Results

In this section, we evaluate  $\beta$ -CROWN in both complete and incomplete verification settings. Our code is available at <https://github.com/KaidiXu/Beta-CROWN>.

### 4.1. Comparison to Incomplete Verifiers

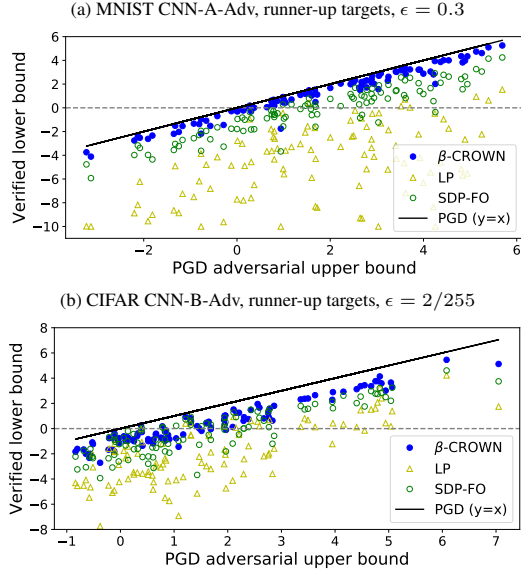
We can early stop  $\beta$ -CROWN BaBSR within a certain time threshold and perform incomplete verification. In this section, we verify  $\ell_\infty$  robustness of two PGD adversarially trained MNIST and CIFAR10 models reported in (Dathathri et al., 2020) (model details in Appendix C). These models are challenging for incomplete verifiers, and typically an expensive semidefinite programming (SDP) based incomplete verifier must be used to verify non-trivial robustness. We show that  $\beta$ -CROWN BaBSR significantly outperforms existing incomplete verifiers including the state-of-the-art SDP based verifier on GPUs, SDP-FO (Dathathri et al., 2020).

**Tightness of verification.** In Figure 1, we compare the tightness of verification bounds against SDP-FO following the similar evaluation setting in (Dathathri et al., 2020). Specifically, we use the verification objective  $f(x) := z_y^{(L)}(x) - z_{y'}^{(L)}(x)$ , where  $z^{(L)}$  is the logit layer output,  $y$  is the true label of image and  $y'$  is the runner-up label under benign settings. For each test image, PGD attack (Madry et al., 2018) can provide an adversarial upper bound of the optimal objective  $f^* \leq \bar{f}$ . Verifiers, on the other hand, can provide a verified lower bound  $\underline{f} \leq f^*$ . The image is said to be verified given targeted label  $y'$  if  $\underline{f} \geq 0$ . The closer the verified objective  $\underline{f}$  is to its PGD upper bound  $\bar{f}$  (closer to line  $y = x$  in Figure 1), the tighter the verification is. Figure 1 shows that on both PGD adversarially trained networks,  $\beta$ -CROWN BaBSR consistently outperforms SDP-FO for all 100 random test images. Importantly, for each point on the plot,  $\beta$ -CROWN BaBSR needs only 3 minutes while SDP-FO needs 178 minutes on average. We are at least 47 times faster than the state-of-the-art SDP-FO while obtaining remarkably tighter bounds. Linear programming (LP) produces much looser bounds than  $\beta$ -CROWN BaBSR and SDP-FO. We do not include other linear relaxation based verifiers such as (Wong & Kolter, 2018) because they are weaker (Salman et al., 2019) than LP.

**Verified accuracy.** In Table 1, we compare the verified accuracy and verification time on adversarially trained MNIST and CIFAR-10 models using existing incomplete verifiers on 100 random testing images. Due to resource limitations<sup>1</sup>,

<sup>1</sup>For each target label of each sampled image, SDP-FO needs about 3 hours on average and thus needs a total of 2,700 GPU hours for 100 testing images. We thus obtain the same pretrained models from Dathathri et al. (2020) and reuse their results.

Figure 1. Verified lower bound on  $f(x)$  v.s. the adversarial upper bound on  $f(x)$  found by PGD. A lower bound closer to the upper bound (closer to the line  $y = x$ ) is better.  $\beta$ -CROWN achieves tighter verification across all examples than the SOTA incomplete verifier SDP-FO; additionally  $\beta$ -CROWN uses 3 mins to produce each point and SDP-FO requires roughly 3 hours per point.



we directly quote the verified accuracy from (Dathathri et al., 2020) on the same models. On these adversarially trained models, weaker incomplete verifiers like Wong & Kolter (2018), CROWN, and LP cannot obtain good verified accuracy especially on the MNIST model with a large  $\epsilon = 0.3$ . SDP-FO provides non-trivial verified errors on both models with very high time cost.  $\beta$ -CROWN BaBSR is 60 times faster than SDP-FO on average and achieves significantly better verified accuracy, especially on MNIST at  $\epsilon = 0.3$ : our verified accuracy (66%) is close to PGD accuracy (78%), and the gap between verified accuracy and PGD accuracy (12%) is much smaller than that of SDP-FO (35%).

## 4.2. Comparison to Complete Verifiers

We evaluate our performance on complete verification on the dataset provided in (De Palma et al., 2021). The dataset contains three CIFAR-10 models (Base, Wide and Deep) with 100 examples each. Each data example is associated with an  $\epsilon$  and a target label for verification (referred to as a *property* to verify). The verification problem is to check  $\ell_\infty$  robustness with norm  $\epsilon$  and the target label within a specific time constraint. The details of neural network structures and experimental setups can be found in Appendix C.

We compare against multiple baselines for complete verification: (1) BABSR (Bunel et al., 2020b), a BaB and LP based verifier using a simple ReLU split heuristic; (2) MIP-PLANET (Ehlers, 2017), a customized MIP solver for NN verification where unstable ReLU neurons are randomly selected for split; (3) GNN-ONLINE (Lu & Kumar, 2020)

Table 1. Verified accuracy obtained by different incomplete solvers on 100 random test images. For each image,  $\beta$ -CROWN needs only 27 minutes while SDP-FO needs > 21 hours. Other incomplete verifiers are not powerful enough for adversarially trained models.

Dataset		MNIST $\epsilon = 0.3$	CIFAR10 $\epsilon = 2/255$
Perturbation norm ( $\ell_\infty$ )			
Model (from Dathathri et al. (2020))		CNN-A-Adv	CNN-B-Adv
Number of model parameters		166,406	2,118,856
Accuracy	Norminal PGD	98.0% 78.0%	78.0% 63.0%
Verified Accuracy	Wong & Kolter (2018) CROWN LP <sup>1</sup> SDP-FO <sup>2</sup> $\beta$ -CROWN BaBSR	0% 1.0% 1.0% 43.4% <b>66.0%</b>	10.0% 22.0% 16.0% 32.8% <b>35.0%</b>
Avg. Verified Time/Sample	Wong & Kolter (2018) CROWN LP SDP-FO $\beta$ -CROWN BaBSR	0.02 mins 0.02 mins 3.35 mins 1,274.38 mins 27.00 mins	0.11 mins 0.11 mins 64.30 mins 1,926.21 mins 27.00 mins

<sup>1</sup> LPs constructed using intermediate bounds from Wong & Kolter.

<sup>2</sup> From 500 test images as reported in (Dathathri et al., 2020).

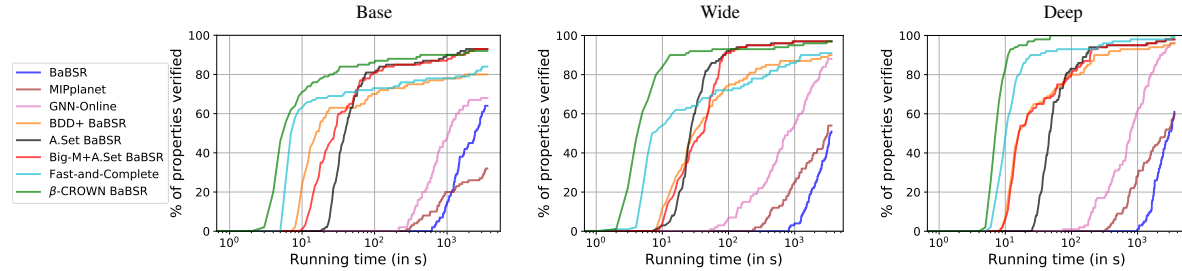
a BaB and LP based verifiers using a learned Graph Neural Network (GNN) to guide the ReLU splits. (4) BDD+ BABSR (Bunel et al., 2020a), a verification framework based on Lagrangian decomposition and runs on GPUs (5) A.SET BABSR and (6)BIG-M+A.SET BABSR (De Palma et al., 2021) are very recent dual-space verifiers on GPUs with a tighter linear relaxation than LP. (7) FAST-AND-COMPLETE (Xu et al., 2021), which uses CROWN on GPUs as the incomplete verifier in BaB without neuron split constraints. All methods use 1 CPU with 1 GPU. The timeout threshold is 3,600 seconds.

In Table 2, we report the *median* verification time and median number of branches on the three models. We do not use average time because it is heavily biased towards timed out examples (we report them in Appendix C).  $\beta$ -CROWN BABSR can achieve the fastest median running time compared to other baselines with minimal timeouts. When compared to methods with similar timeout rates such as A.SET BABSR,  $\beta$ -CROWN BABSR is at least twice and up to 7x faster. Although Xu et al. (2021) is relatively fast (still 60% to 100% slower than us), they have significantly more timeouts because they use CROWN as the incomplete verifier which cannot handle neuron split constraints, leading to undetected infeasible splits and high timeout rates. Our benefits are more clearly shown in Figure 2, where we solve most examples under 10 seconds and most other verifiers can only verify a small portion or none of the properties within 10 seconds. We provide additional comparisons to other complete and incomplete solvers in Appendix C.2.

**Table 2.** Median runtime and median number of branches on three models over 100 properties. We report the median because the average runtime significantly biases towards timed out samples (3600s) while most samples are solved by us within 10s, making the metric ineffective. FAST-AND-COMPLETE is faster than many baselines but has a high timeout rate due to the lack of split constraint checking. Our  $\beta$ -CROWN BABSR is faster than all baselines and also achieves low timeout rates. We include average metrics in Appendix C.

Method	CIFAR-10 Base			CIFAR-10 Wide			CIFAR-10 Deep		
	median time(s)	branches	%timeout	median time(s)	branches	%timeout	median time(s)	branches	%timeout
BABSR	2421.03	729.95	36.00	3490.12	573.46	49.00	2982.27	398.32	39.00
MIPPLANET	3600.00	-	68.00	3129.05	-	46.00	2606.58	-	40.00
GNN-ONLINE	1198.55	400.17	33.00	890.02	281.98	15.00	793.91	101.58	4.00
BDD+ BABSR	16.01	2866.08	20.88	30.05	4414.64	10.00	15.53	870.02	4.00
A.SET BABSR	39.74	813.55	<b>7.00</b>	27.68	174.16	<b>3.00</b>	45.96	401.04	2.00
BIG-M+A.SET BABSR	28.56	2839.40	<b>7.00</b>	40.84	2123.96	<b>3.00</b>	17.5	955.20	2.00
FAST-AND-COMPLETE	8.85	499.14	17.00	10.17	354.82	9.00	10.28	101.55	1.00
$\beta$ -CROWN BABSR	<b>5.11</b>	<b>327.19</b>	8.00	<b>4.05</b>	<b>101.41</b>	<b>3.00</b>	<b>7.25</b>	<b>58.75</b>	<b>0.00</b>

**Figure 2.** Cactus plots for our method and other baselines for CIFAR-10 Base, Wide and Deep models. We plot the percentage of solved properties with growing running time.  $\beta$ -CROWN BABSR clearly leads in all three settings and solves most properties within 10 seconds.



## 5. Related Work

Early complete verifiers relied on existing solvers (Katz et al., 2017; Ehlers, 2017; Huang et al., 2017; Dutta et al., 2018; Tjeng et al., 2019) but limited to very small problem instances. BaB based method was proposed to better exploit the network structure (Bunel et al., 2018), including recent works (Bunel et al., 2018; Wang et al., 2018b; Lu & Kumar, 2020; Botoeva et al., 2020), with LP-based incomplete verifier for bounding and ReLU splits for branching. Input domain branching was also considered in (Wang et al., 2018c; Royo et al., 2019; Anderson et al., 2019) but they are limited by input dimensions (Bunel et al., 2018). Most traditional complete verifiers typically need hours to verify one example on networks with a few thousand neurons.

Recently, instead of using LP for bounding, a few approaches have been proposed to use efficient iterative solvers based on bound propagation methods on GPUs. Bunel et al. (2020a) decomposed problem layer by layer, solved each layer in a closed form on GPUs, and used Lagrangian to enforce consistency between layers. However, their formulation only has the same power as LP and needs many iterations to converge. De Palma et al. (2021) used a dual-space verifier and a tighter linear relaxation (Anderson et al., 2020; Tjandraatmadja et al., 2020) than LP at a cost of exponentially many constraints. The complexity of this relaxation disallows the optimization of intermediate layer bounds and makes it less efficient than  $\beta$ -CROWN. Xu et al. (2020) parallelized CROWN on GPUs, but it fails to handle neuron split constraints, leading to suboptimal efficiency.

For incomplete verification, Salman et al. (2019) shows the

inherent limitation of using per-neuron convex relaxations for verification problem. Singh et al. (2019a) broke this barrier by relaxing multiple neurons; Tjandraatmadja et al. (2020); De Palma et al. (2021) used a tighter linear relaxation for a layer of ReLU neurons together, but they must choose from exponentially many linear hyperplanes. SDP based relaxations (Raghunathan et al., 2018; Fazlyab et al., 2020; Dvijotham et al., 2020; Dathathri et al., 2020) typically produce tighter bounds than linear relaxations but with a significantly higher computational cost. In this work, we impose neuron split constraints using  $\beta$ -CROWN, break this barrier using BaB, and outperform the tight SDP relaxation based solvers in both runtime and tightness.

Additionally, another line of works trains networks to increase verified accuracy, typically relying on cheap incomplete verifiers at training time, like linear relaxations (Wong & Kolter, 2018; Wang et al., 2018a; Mirman et al., 2018; Wong et al., 2018), interval bound propagation (Gowal et al., 2018; Mirman et al., 2018) or hybrid methods (Zhang et al., 2020; Balunovic & Vechev, 2020). Only these verification-customized networks can have reasonable verified accuracy. In contrast,  $\beta$ -CROWN with BaB can give non-trivial verified accuracy on relatively large networks agnostic to verification, where very few existing verifiers can do.

## 6. Conclusion

We proposed  $\beta$ -CROWN, a new bound propagation method that can fully encode the neuron split constraints introduced in BaB. It can jointly optimize its free variables with intermediate layer bounds and outperform typical LP verifiers while

enjoying the efficiency on GPUs. We show that BaB-based complete verifier using  $\beta$ -CROWN outperforms all state-of-the-art complete verifiers and is almost  $1000\times$  faster than LP-based ones. By early stopping our complete verifier, we can obtain much higher verified accuracy than state-of-the-art incomplete verifiers within at least  $47\times$  less verification time on adversarially trained neural networks, representing a substantial leap forward in the accuracy and scalability of verification for verification-agnostic networks.

## References

Anderson, G., Pailoor, S., Dillig, I., and Chaudhuri, S. Optimization and abstraction: A synergistic approach for analyzing neural network robustness. In *Proceedings of the 40th ACM SIGPLAN Conference on Programming Language Design and Implementation*, pp. 731–744, 2019.

Anderson, R., Huchette, J., Tjandraatmadja, C., and Vielma, J. P. Strong convex relaxations and mixed-integer programming formulations for trained neural networks. *Mathematical Programming*, 2020.

Balunovic, M. and Vechev, M. Adversarial training and provable defenses: Bridging the gap. In *International Conference on Learning Representations*, 2020.

Botoeva, E., Kouvaros, P., Kronqvist, J., Lomuscio, A., and Misener, R. Efficient verification of relu-based neural networks via dependency analysis. In *AAAI*, 2020.

Bunel, R., De Palma, A., Desmaison, A., Dvijotham, K., Kohli, P., Torr, P. H. S., and Kumar, M. P. Lagrangian decomposition for neural network verification. *Conference on Uncertainty in Artificial Intelligence (UAI) 2020*, 2020a.

Bunel, R., Lu, J., Turkaslan, I., Kohli, P., Torr, P., and Mudigonda, P. Branch and bound for piecewise linear neural network verification. *Journal of Machine Learning Research*, 21(2020), 2020b.

Bunel, R. R., Turkaslan, I., Torr, P., Kohli, P., and Mudigonda, P. K. A unified view of piecewise linear neural network verification. In *Advances in Neural Information Processing Systems*, pp. 4790–4799, 2018.

Dathathri, S., Dvijotham, K., Kurakin, A., Raghunathan, A., Uesato, J., Bunel, R. R., Shankar, S., Steinhardt, J., Goodfellow, I., Liang, P. S., et al. Enabling certification of verification-agnostic networks via memory-efficient semidefinite programming. *Advances in Neural Information Processing Systems*, 33, 2020.

De Palma, A., Behl, H. S., Bunel, R., Torr, P. H. S., and Kumar, M. P. Scaling the convex barrier with active sets. *International Conference on Learning Representations*, 2021.

Dutta, S., Jha, S., Sankaranarayanan, S., and Tiwari, A. Output range analysis for deep feedforward neural networks. In *NASA Formal Methods Symposium*, pp. 121–138. Springer, 2018.

Dvijotham, K., Stanforth, R., Gowal, S., Mann, T., and Kohli, P. A dual approach to scalable verification of deep networks. *UAI*, 2018.

Dvijotham, K. D., Stanforth, R., Gowal, S., Qin, C., De, S., and Kohli, P. Efficient neural network verification with exactness characterization. In *Uncertainty in Artificial Intelligence*, pp. 497–507. PMLR, 2020.

Ehlers, R. Formal verification of piece-wise linear feed-forward neural networks. In *International Symposium on Automated Technology for Verification and Analysis*, pp. 269–286. Springer, 2017.

Fazlyab, M., Morari, M., and Pappas, G. J. Safety verification and robustness analysis of neural networks via quadratic constraints and semidefinite programming. *IEEE Transactions on Automatic Control*, 2020.

Gehr, T., Mirman, M., Drachsler-Cohen, D., Tsankov, P., Chaudhuri, S., and Vechev, M. Ai2: Safety and robustness certification of neural networks with abstract interpretation. In *2018 IEEE Symposium on Security and Privacy (SP)*, pp. 3–18. IEEE, 2018.

Gowal, S., Dvijotham, K., Stanforth, R., Bunel, R., Qin, C., Uesato, J., Mann, T., and Kohli, P. On the effectiveness of interval bound propagation for training verifiably robust models. *arXiv preprint arXiv:1810.12715*, 2018.

Huang, X., Kwiatkowska, M., Wang, S., and Wu, M. Safety verification of deep neural networks. In *International Conference on Computer Aided Verification*, pp. 3–29. Springer, 2017.

Katz, G., Barrett, C., Dill, D. L., Julian, K., and Kochenderfer, M. J. Reluplex: An efficient smt solver for verifying deep neural networks. In *International Conference on Computer Aided Verification*, pp. 97–117. Springer, 2017.

Kingma, D. P. and Ba, J. Adam: A method for stochastic optimization. *arXiv preprint arXiv:1412.6980*, 2014.

Lu, J. and Kumar, M. P. Neural network branching for neural network verification. *International Conference on Learning Representation (ICLR)*, 2020.

Madry, A., Makelov, A., Schmidt, L., Tsipras, D., and Vladu, A. Towards deep learning models resistant to adversarial attacks. In *ICLR*, 2018.

Mirman, M., Gehr, T., and Vechev, M. Differentiable abstract interpretation for provably robust neural networks.

In *International Conference on Machine Learning*, pp. 3575–3583, 2018.

Raghunathan, A., Steinhardt, J., and Liang, P. S. Semidefinite relaxations for certifying robustness to adversarial examples. In *Advances in Neural Information Processing Systems*, pp. 10877–10887, 2018.

Royo, V. R., Calandra, R., Stipanovic, D. M., and Tomlin, C. Fast neural network verification via shadow prices. *arXiv preprint arXiv:1902.07247*, 2019.

Salman, H., Yang, G., Zhang, H., Hsieh, C.-J., and Zhang, P. A convex relaxation barrier to tight robustness verification of neural networks. In *Advances in Neural Information Processing Systems 32*, pp. 9832–9842, 2019.

Shi, Z., Zhang, H., Chang, K.-W., Huang, M., and Hsieh, C.-J. Robustness verification for transformers. In *International Conference on Learning Representations*, 2020.

Singh, G., Ganvir, R., Püschel, M., and Vechev, M. Beyond the single neuron convex barrier for neural network certification. In *Advances in Neural Information Processing Systems*, pp. 15072–15083, 2019a.

Singh, G., Gehr, T., Püschel, M., and Vechev, M. An abstract domain for certifying neural networks. *Proceedings of the ACM on Programming Languages*, 3(POPL):41, 2019b.

Tjandraatmadja, C., Anderson, R., Huchette, J., Ma, W., Patel, K., and Vielma, J. P. The convex relaxation barrier, revisited: Tightened single-neuron relaxations for neural network verification. *arXiv preprint arXiv:2006.14076*, 2020.

Tjeng, V., Xiao, K., and Tedrake, R. Evaluating robustness of neural networks with mixed integer programming. *ICLR*, 2019.

Wang, S., Chen, Y., Abdou, A., and Jana, S. Mixtrain: Scalable training of formally robust neural networks. *arXiv preprint arXiv:1811.02625*, 2018a.

Wang, S., Pei, K., Whitehouse, J., Yang, J., and Jana, S. Efficient formal safety analysis of neural networks. In *Advances in Neural Information Processing Systems*, pp. 6367–6377, 2018b.

Wang, S., Pei, K., Whitehouse, J., Yang, J., and Jana, S. Formal security analysis of neural networks using symbolic intervals. In *27th {USENIX} Security Symposium ({USENIX} Security 18)*, pp. 1599–1614, 2018c.

Wong, E. and Kolter, Z. Provable defenses against adversarial examples via the convex outer adversarial polytope. In *International Conference on Machine Learning*, pp. 5283–5292, 2018.

Wong, E., Schmidt, F., Metzen, J. H., and Kolter, J. Z. Scaling provable adversarial defenses. In *NIPS*, 2018.

Xu, K., Shi, Z., Zhang, H., Wang, Y., Chang, K.-W., Huang, M., Kailkhura, B., Lin, X., and Hsieh, C.-J. Automatic perturbation analysis for scalable certified robustness and beyond. *Advances in Neural Information Processing Systems*, 33, 2020.

Xu, K., Zhang, H., Wang, S., Wang, Y., Jana, S., Lin, X., and Hsieh, C.-J. Fast and complete: Enabling complete neural network verification with rapid and massively parallel incomplete verifiers. *International Conference on Learning Representations*, 2021.

Zhang, H., Weng, T.-W., Chen, P.-Y., Hsieh, C.-J., and Daniel, L. Efficient neural network robustness certification with general activation functions. In *Advances in neural information processing systems*, pp. 4939–4948, 2018.

Zhang, H., Chen, H., Xiao, C., Li, B., Boning, D., and Hsieh, C.-J. Towards stable and efficient training of verifiably robust neural networks. In *International Conference on Learning Representations*, 2020.

## A. Proofs for $\beta$ -CROWN

### A.1. Proofs for deriving $\beta$ -CROWN using bound propagation

Lemma 2.1 is from part of the proof of the main theorem in (Zhang et al., 2018). Here we present it separately to use it as an useful subprocedure for our later proofs.

**Lemma 2.1** (Relaxation of a ReLU layer in CROWN). *Given two vectors  $w, v \in \mathbb{R}^d$ ,  $\mathbf{u} \leq v \leq \mathbf{l}$  (element-wise), we have*

$$w^\top \text{ReLU}(v) \geq w^\top \mathbf{D}v + b',$$

where  $\mathbf{D}$  is a diagonal matrix defined as:

$$\mathbf{D}_{j,j} = \begin{cases} 1, & \text{if } \mathbf{l}_j \geq 0 \\ 0, & \text{if } \mathbf{u}_j \leq 0 \\ \alpha_j, & \text{if } \mathbf{u}_j > 0 > \mathbf{l}_j \text{ and } w_j \geq 0 \\ \frac{\mathbf{u}_j}{\mathbf{u}_j - \mathbf{l}_j}, & \text{if } \mathbf{u}_j > 0 > \mathbf{l}_j \text{ and } w_j < 0, \end{cases} \quad (11)$$

$0 \leq \alpha_j \leq 1$  are free variables,  $b' = w^\top \underline{\mathbf{b}}$  and each element in  $\underline{\mathbf{b}}$  is

$$\underline{\mathbf{b}}_j = \begin{cases} 0, & \text{if } \mathbf{l}_j > 0 \text{ or } \mathbf{u}_j \leq 0 \\ 0, & \text{if } \mathbf{u}_j > 0 > \mathbf{l}_j \text{ and } w_j \geq 0 \\ -\frac{\mathbf{u}_j \mathbf{l}_j}{\mathbf{u}_j - \mathbf{l}_j}, & \text{if } \mathbf{u}_j > 0 > \mathbf{l}_j \text{ and } w_j < 0. \end{cases} \quad (12)$$

*Proof.* For the  $j$ -th ReLU neuron, if  $\mathbf{l}_j \geq 0$ , then  $\text{ReLU}(v_j) = v_j$ ; if  $\mathbf{u}_j < 0$ , then  $\text{ReLU}(v_j) = 0$ . For the case of  $\mathbf{l}_j < 0 < \mathbf{u}_j$ , the ReLU function can be linearly upper and lower bounded within this range:

$$\alpha_j v_j \leq \text{ReLU}(v_j) \leq \frac{\mathbf{u}_j}{\mathbf{u}_j - \mathbf{l}_j} (v_j - \mathbf{l}_j) \quad \forall \mathbf{l}_j \leq v_j \leq \mathbf{u}_j$$

where  $0 \leq \alpha_j \leq 1$  is a free variable - any value between 0 and 1 produces a valid lower bound. To lower bound  $w^\top \text{ReLU}(v) = \sum_j w_j \text{ReLU}(v_j)$ , for each term in this summation, we take the lower bound of  $\text{ReLU}(v_j)$  if  $w_j$  is positive and take the upper bound of  $\text{ReLU}(v_j)$  if  $w_j$  is negative (reflected in the definitions of  $\mathbf{D}$  and  $\underline{\mathbf{b}}$ ). This conservative choice allows us to always obtain a lower bound  $\forall \mathbf{l} \leq v \leq \mathbf{u}$ :

$$\sum_j w_j \text{ReLU}(v_j) \geq \sum_j w_j (\mathbf{D}_{j,j} v_j + \underline{\mathbf{b}}_j) = w^\top \mathbf{D}v + w^\top \underline{\mathbf{b}} = w^\top \mathbf{D}v + b'$$

where  $\mathbf{D}_{j,j}$  and  $\underline{\mathbf{b}}_j$  are defined in Eq. 11 and Eq. 12 representing the lower or upper bounds of ReLU.  $\square$

Before proving our main theorem (Theorem 3.1), we first define matrix  $\Omega$ , which is the product of a series of model weights  $\mathbf{W}$  and “weights” for relaxed ReLU layers  $\mathbf{D}$ :

**Definition A.1.** *Given a set of matrices  $\mathbf{W}^{(2)}, \dots, \mathbf{W}^{(L)}$  and  $\mathbf{D}^{(1)}, \dots, \mathbf{D}^{(L-1)}$ , we define a recursive function  $\Omega(k, i)$  for  $1 \leq i \leq k \leq L$  as*

$$\Omega(i, i) = \mathbf{I}, \quad \Omega(k+1, i) = \mathbf{W}^{(k+1)} \mathbf{D}^{(k)} \Omega(k, i)$$

For example,  $\Omega(3, 1) = \mathbf{W}^{(3)} \mathbf{D}^{(2)} \mathbf{W}^{(2)} \mathbf{D}^{(1)}$ ,  $\Omega(5, 2) = \mathbf{W}^{(5)} \mathbf{D}^{(4)} \mathbf{W}^{(4)} \mathbf{D}^{(3)} \mathbf{W}^{(3)} \mathbf{D}^{(2)}$ . Now we present our main theorem with each term explicitly written:

**Theorem 3.1** ( $\beta$ -CROWN bound). *Given a  $L$ -layer neural network  $f(x) : \mathbb{R}^{d_0} \rightarrow \mathbb{R}$  with weights  $\mathbf{W}^{(i)}$ , biases  $\mathbf{b}^{(i)}$ , pre-ReLU bounds  $\mathbf{l}^{(i)} \leq z^{(i)} \leq \mathbf{u}^{(i)}$  ( $1 \leq i \leq L$ ), input constraint  $\mathcal{C}$  and split constraint  $\mathcal{Z}$ . We have*

$$\min_{x \in \mathcal{C}, z \in \mathcal{Z}} f(x) \geq \max_{\beta \geq 0} \min_{x \in \mathcal{C}} (\mathbf{a} + \mathbf{P}\beta)^\top x + \mathbf{q}^\top \beta + c, \quad (13)$$

where  $\mathbf{P} \in \mathbb{R}^{d_0 \times (\sum_{i=1}^{L-1} d_i)}$  is a matrix containing blocks  $\mathbf{P} := [\mathbf{P}_1^\top \mathbf{P}_2^\top \dots \mathbf{P}_{L-1}^\top]$ ,  $\mathbf{q} \in \mathbb{R}^{\sum_{i=1}^{L-1} d_i}$  is a vector  $\mathbf{q} := [\mathbf{q}_1^\top \dots \mathbf{q}_{L-1}^\top]^\top$ , and each term is defined as:

$$\mathbf{a} = [\Omega(L, 1) \mathbf{W}^{(1)}]^\top \in \mathbb{R}^{d_0 \times 1} \quad (14)$$

$$\mathbf{P}_i = \mathbf{S}^{(i)} \boldsymbol{\Omega}(i, 1) \mathbf{W}^{(1)} \in \mathbb{R}^{d_i \times d_0}, \quad \forall 1 \leq i \leq L-1 \quad (15)$$

$$\mathbf{q}_i = \sum_{k=1}^i \mathbf{S}^{(i)} \boldsymbol{\Omega}(i, k) \mathbf{b}^{(k)} + \sum_{k=2}^i \mathbf{S}^{(i)} \boldsymbol{\Omega}(i, k) \mathbf{W}^{(k)} \underline{\mathbf{b}}^{(k-1)} \in \mathbb{R}^{d_i}, \quad \forall 1 \leq i \leq L-1 \quad (16)$$

$$c = \sum_{i=1}^L \boldsymbol{\Omega}(L, i) \mathbf{b}^{(i)} + \sum_{i=2}^L \boldsymbol{\Omega}(L, i) \mathbf{W}^{(i)} \underline{\mathbf{b}}^{(i-1)} \quad (17)$$

diagonal matrices  $\mathbf{D}^{(i)}$  and vector  $\underline{\mathbf{b}}^{(i)}$  are determined by the relaxation of ReLU neurons, and  $\mathbf{A}^{(i)} \in \mathbb{R}^{1 \times d_i}$  represents the linear relationship between  $f(x)$  and  $\hat{z}^{(i)}$ .  $\mathbf{D}^{(i)}$  and  $\underline{\mathbf{b}}^{(i)}$  depend on  $\mathbf{A}^{(i)}$ ,  $\mathbf{l}^{(i)}$  and  $\mathbf{u}^{(i)}$ :

$$\mathbf{D}_{j,j}^{(i)} = \begin{cases} 1, & \text{if } \mathbf{l}_j^{(i)} \geq 0 \text{ or } j \in \mathcal{Z}^{+(i)} \\ 0, & \text{if } \mathbf{u}_j^{(i)} \leq 0 \text{ or } j \in \mathcal{Z}^{-(i)} \\ \boldsymbol{\alpha}_j, & \text{if } \mathbf{u}_j^{(i)} > 0 > \mathbf{l}_j^{(i)} \text{ and } j \notin \mathcal{Z}^{+(i)} \cup \mathcal{Z}^{-(i)} \text{ and } \mathbf{A}_{1,j}^{(i)} \geq 0 \\ \frac{\mathbf{u}_j^{(i)}}{\mathbf{u}_j^{(i)} - \mathbf{l}_j^{(i)}}, & \text{if } \mathbf{u}_j^{(i)} > 0 > \mathbf{l}_j^{(i)} \text{ and } j \notin \mathcal{Z}^{+(i)} \cup \mathcal{Z}^{-(i)} \text{ and } \mathbf{A}_{1,j}^{(i)} < 0 \end{cases} \quad (18)$$

$$\underline{\mathbf{b}}_j^{(i)} = \begin{cases} 0, & \text{if } \mathbf{l}_j^{(i)} > 0 \text{ or } \mathbf{u}_j^{(i)} \leq 0 \text{ or } j \in \mathcal{Z}^{+(i)} \cup \mathcal{Z}^{-(i)} \\ 0, & \text{if } \mathbf{u}_j^{(i)} > 0 > \mathbf{l}_j^{(i)} \text{ and } j \notin \mathcal{Z}^{+(i)} \cup \mathcal{Z}^{-(i)} \text{ and } \mathbf{A}_{1,j}^{(i)} \geq 0 \\ -\frac{\mathbf{u}_j^{(i)} \mathbf{l}_j^{(i)}}{\mathbf{u}_j^{(i)} - \mathbf{l}_j^{(i)}}, & \text{if } \mathbf{u}_j^{(i)} > 0 > \mathbf{l}_j^{(i)} \text{ and } j \notin \mathcal{Z}^{+(i)} \cup \mathcal{Z}^{-(i)} \text{ and } \mathbf{A}_{1,j}^{(i)} < 0 \end{cases} \quad (19)$$

$$\mathbf{A}^{(i)} = \begin{cases} \mathbf{W}^{(L)}, & i = L-1 \\ (\mathbf{A}^{(i+1)} \mathbf{D}^{(i+1)} + \boldsymbol{\beta}^{(i+1)\top} \mathbf{S}^{(i+1)}) \mathbf{W}^{(i+1)}, & 0 \leq i \leq L-2 \end{cases} \quad (20)$$

*Proof.* We prove this theorem by induction: assuming we know the bounds with respect to layer  $\hat{z}^{(m)}$ , we derive bounds for  $\hat{z}^{(m-1)}$  until we reach  $m = 0$  and by definition  $\hat{z}^{(0)} = x$ . We first define a set of matrices and vectors  $\mathbf{a}^{(m)}$ ,  $\mathbf{P}^{(m)}$ ,  $\mathbf{q}^{(m)}$ ,  $c^{(m)}$ , where  $\mathbf{P}^{(m)} \in \mathbb{R}^{d_m \times (\sum_{i=m+1}^{L-1} d_i)}$  is a matrix containing blocks  $\mathbf{P} := \left[ \mathbf{P}_{m+1}^{(m)\top} \cdots \mathbf{P}_{L-1}^{(m)\top} \right]$ ,  $\mathbf{q} \in \mathbb{R}^{\sum_{i=m+1}^{L-1} d_i}$  is a vector  $\mathbf{q} := \left[ \mathbf{q}_{m+1}^{(m)\top} \cdots \mathbf{q}_{L-1}^{(m)\top} \right]^\top$ , and each term is defined as:

$$\mathbf{a}^{(m)} = \left[ \boldsymbol{\Omega}(L, m+1) \mathbf{W}^{(m+1)} \right]^\top \in \mathbb{R}^{d_m \times 1} \quad (21)$$

$$\mathbf{P}_i^{(m)} = \mathbf{S}^{(i)} \boldsymbol{\Omega}(i, m+1) \mathbf{W}^{(m+1)} \in \mathbb{R}^{d_i \times d_m}, \quad \forall m+1 \leq i \leq L-1 \quad (22)$$

$$\mathbf{q}_i^{(m)} = \sum_{k=m+1}^i \mathbf{S}^{(i)} \boldsymbol{\Omega}(i, k) \mathbf{b}^{(k)} + \sum_{k=m+2}^i \mathbf{S}^{(i)} \boldsymbol{\Omega}(i, k) \mathbf{W}^{(k)} \underline{\mathbf{b}}^{(k-1)} \in \mathbb{R}^{d_m}, \quad \forall m+1 \leq i \leq L-1 \quad (23)$$

$$c^{(m)} = \sum_{i=m+1}^L \boldsymbol{\Omega}(L, i) \mathbf{b}^{(i)} + \sum_{i=m+2}^L \boldsymbol{\Omega}(L, i) \mathbf{W}^{(i)} \underline{\mathbf{b}}^{(i-1)} \quad (24)$$

and we claim that

$$\min_{\substack{x \in \mathcal{C} \\ z \in \mathcal{Z}}} f(x) \geq \max_{\substack{\tilde{\boldsymbol{\beta}}^{(m+1)} \geq 0 \\ \tilde{z}^{(m)} \in \tilde{\mathcal{Z}}^{(m)}}} (\mathbf{a}^{(m)} + \mathbf{P}^{(m)} \tilde{\boldsymbol{\beta}}^{(m+1)})^\top \hat{z}^{(m)} + \mathbf{q}^{(m)\top} \tilde{\boldsymbol{\beta}}^{(m+1)} + c^{(m)} \quad (25)$$

where  $\tilde{\boldsymbol{\beta}}^{(m+1)} := [\boldsymbol{\beta}^{(m+1)\top} \cdots \boldsymbol{\beta}^{(L-1)\top}]^\top$  concatenating all  $\boldsymbol{\beta}^{(i)}$  variables up to layer  $m+1$ .

For the base case  $m = L-1$ , we simply have

$$\min_{x \in \mathcal{C}, z \in \mathcal{Z}} f(x) = \min_{x \in \mathcal{C}, z \in \mathcal{Z}} \mathbf{W}^{(L)} \hat{z}^{(L-1)} + \mathbf{b}^{(L)}.$$

No maximization is needed and  $\mathbf{a}^{(m)} = [\boldsymbol{\Omega}(L, L) \mathbf{W}^{(L)}]^\top = \mathbf{W}^{(L)\top}$ ,  $c^{(m)} = \sum_{i=L}^L \boldsymbol{\Omega}(L, i) \mathbf{b}^{(i)} = \mathbf{b}^{(L)}$ . Other terms are zero.

In Section 3.1 we have shown the intuition of the proof by demonstrating how to derive the bounds from layer  $\hat{z}^{(L-1)}$  to  $\hat{z}^{(L-2)}$ . The case for  $m = L - 2$  is presented in Eq. 4.

Now we show the induction from  $\hat{z}^{(m)}$  to  $\hat{z}^{(m-1)}$ . Starting from Eq. 25, since  $\hat{z}^{(m)} = \text{ReLU}(z^{(m)})$  we apply Lemma 2.1 by setting  $w = [\mathbf{a}^{(m)} + \mathbf{P}^{(m)} \tilde{\boldsymbol{\beta}}^{(m+1)}]^\top := \mathbf{A}^{(m)}$ . It is easy to show that  $\mathbf{A}^{(m)}$  can also be equivalently and recursively defined in Eq. 20 (see Lemma A.2). Based on Lemma 2.1 we have  $\mathbf{D}^{(m)}$  and  $\underline{\mathbf{b}}^{(m)}$  defined as in Eq. 18 and Eq. 19, so Eq. 25 becomes

$$\begin{aligned} \min_{\substack{x \in \mathcal{C} \\ z \in \mathcal{Z}}} f(x) &\geq \max_{\tilde{\boldsymbol{\beta}}^{(m+1)} \geq 0} \min_{\substack{x \in \mathcal{C} \\ \hat{z}^{(m)} \in \hat{\mathcal{Z}}^{(m)}}} (\mathbf{a}^{(m)} + \mathbf{P}^{(m)} \tilde{\boldsymbol{\beta}}^{(m+1)})^\top \mathbf{D}^{(m)} z^{(m)} \\ &\quad + (\mathbf{a}^{(m)} + \mathbf{P}^{(m)} \tilde{\boldsymbol{\beta}}^{(m+1)})^\top \underline{\mathbf{b}}^{(m)} + \mathbf{q}^{(m)\top} \tilde{\boldsymbol{\beta}}^{(m+1)} + c^{(m)} \end{aligned} \quad (26)$$

Note that when we apply Lemma 2.1, for  $j \in \mathcal{Z}^{+(i)}$  (positive split) we simply treat the neuron  $j$  as if  $\mathbf{l}_j^{(i)} \geq 0$ , and for  $j \in \mathcal{Z}^{-(i)}$  (negative split) we simply treat the neuron  $j$  as if  $\mathbf{u}_j^{(i)} \leq 0$ . Now we add the multiplier  $\boldsymbol{\beta}^{(m)}$  to  $z^{(m)}$  to enforce per-neuron split constraints:

$$\begin{aligned} \min_{\substack{x \in \mathcal{C} \\ z \in \mathcal{Z}}} f(x) &\geq \max_{\tilde{\boldsymbol{\beta}}^{(m+1)} \geq 0} \min_{\substack{x \in \mathcal{C} \\ \hat{z}^{(m-1)} \in \hat{\mathcal{Z}}^{(m-1)}}} \max_{\boldsymbol{\beta}^{(m)} \geq 0} (\mathbf{a}^{(m)} + \mathbf{P}^{(m)} \tilde{\boldsymbol{\beta}}^{(m+1)})^\top \mathbf{D}^{(m)} z^{(m)} + \boldsymbol{\beta}^{(m)\top} \mathbf{S}^{(m)} z^{(m)} \\ &\quad + (\mathbf{a}^{(m)} + \mathbf{P}^{(m)} \tilde{\boldsymbol{\beta}}^{(m+1)})^\top \underline{\mathbf{b}}^{(m)} + \mathbf{q}^{(m)\top} \tilde{\boldsymbol{\beta}}^{(m+1)} + c^{(m)} \\ &\geq \max_{\tilde{\boldsymbol{\beta}}^{(m)} \geq 0} \min_{\substack{x \in \mathcal{C} \\ \hat{z}^{(m-1)} \in \hat{\mathcal{Z}}^{(m-1)}}} (\mathbf{a}^{(m)\top} \mathbf{D}^{(m)} + \tilde{\boldsymbol{\beta}}^{(m+1)\top} \mathbf{P}^{(m)\top} \mathbf{D}^{(m)} + \boldsymbol{\beta}^{(m)\top} \mathbf{S}^{(m)}) z^{(m)} \\ &\quad + (\mathbf{a}^{(m)} + \mathbf{P}^{(m)} \tilde{\boldsymbol{\beta}}^{(m+1)})^\top \underline{\mathbf{b}}^{(m)} + \mathbf{q}^{(m)\top} \tilde{\boldsymbol{\beta}}^{(m+1)} + c^{(m)} \end{aligned}$$

Similar to what we did in Eq. 3, we swap the min and max in the second inequality due to weak duality, such that every maximization on  $\boldsymbol{\beta}^{(i)}$  is before min. Then, we substitute  $\hat{z}^{(m)} = \mathbf{W}^{(m)} \hat{z}^{(m-1)} + \mathbf{b}^{(m)}$  and obtain:

$$\begin{aligned} \min_{\substack{x \in \mathcal{C} \\ z \in \mathcal{Z}}} f(x) &\geq \max_{\tilde{\boldsymbol{\beta}}^{(m)} \geq 0} \min_{\substack{x \in \mathcal{C} \\ \hat{z}^{(m-1)} \in \hat{\mathcal{Z}}^{(m-1)}}} (\mathbf{a}^{(m)\top} \mathbf{D}^{(m)} + \tilde{\boldsymbol{\beta}}^{(m+1)\top} \mathbf{P}^{(m)\top} \mathbf{D}^{(m)} + \boldsymbol{\beta}^{(m)\top} \mathbf{S}^{(m)})^\top \mathbf{W}^{(m)} \hat{z}^{(m-1)} \\ &\quad + (\mathbf{a}^{(m)\top} \mathbf{D}^{(m)} + \tilde{\boldsymbol{\beta}}^{(m+1)\top} \mathbf{P}^{(m)\top} \mathbf{D}^{(m)} + \boldsymbol{\beta}^{(m)\top} \mathbf{S}^{(m)})^\top \mathbf{b}^{(m)} + (\mathbf{a}^{(m)} + \mathbf{P}^{(m)} \tilde{\boldsymbol{\beta}}^{(m+1)})^\top \underline{\mathbf{b}}^{(m)} + \mathbf{q}^{(m)\top} \tilde{\boldsymbol{\beta}}^{(m+1)} + c^{(m)} \\ &= \left[ \underbrace{[\mathbf{a}^{(m)\top} \mathbf{D}^{(m)} \mathbf{W}^{(m)}]^\top}_{\mathbf{a}'^\top} + \underbrace{(\tilde{\boldsymbol{\beta}}^{(m+1)\top} \mathbf{P}^{(m)\top} \mathbf{D}^{(m)} \mathbf{W}^{(m)} + \boldsymbol{\beta}^{(m)\top} \mathbf{S}^{(m)} \mathbf{W}^{(m)})^\top}_{\mathbf{P}' \tilde{\boldsymbol{\beta}}^{(m)\top}} \right]^\top \hat{z}^{(m-1)} \\ &\quad + \underbrace{((\mathbf{P}^{(m)\top} \mathbf{D}^{(m)} \mathbf{b}^{(m)} + \mathbf{P}^{(m)\top} \underline{\mathbf{b}}^{(m)} + \mathbf{q}^{(m)\top} \tilde{\boldsymbol{\beta}}^{(m+1)} + (\mathbf{S}^{(m)\top} \mathbf{b}^{(m)})^\top \boldsymbol{\beta}^{(m)})^\top + \underbrace{\mathbf{a}^{(m)\top} \mathbf{D}^{(m)} \mathbf{b}^{(m)} + \mathbf{a}^{(m)\top} \underline{\mathbf{b}}^{(m)} + c^{(m)}}_{\mathbf{q}'^\top \tilde{\boldsymbol{\beta}}^{(m)\top}}} \end{aligned}$$

Now we evaluate each term  $\mathbf{a}'$ ,  $\mathbf{P}'$ ,  $\mathbf{q}'$  and  $c'$  and show the induction holds. For  $\mathbf{a}'$  and  $\mathbf{q}'$  we have:

$$\mathbf{a}' = [\mathbf{a}^{(m)\top} \mathbf{D}^{(m)} \mathbf{W}^{(m)}]^\top = [\boldsymbol{\Omega}(L, m+1) \mathbf{W}^{(m+1)} \mathbf{D}^{(m)} \mathbf{W}^{(m)}]^\top = [\boldsymbol{\Omega}(L, m) \mathbf{W}^{(m)}]^\top = \mathbf{a}^{(m-1)}$$

$$\begin{aligned}
c' &= c^{(m)} + \boldsymbol{\Omega}(L, m+1) \mathbf{W}^{(m+1)} \mathbf{D}^{(m)} \mathbf{b}^{(m)} + \boldsymbol{\Omega}(L, m+1) \mathbf{W}^{(m+1)} \underline{\mathbf{b}}^{(m)} \\
&= \sum_{i=m+1}^L \boldsymbol{\Omega}(L, i) \mathbf{b}^{(i)} + \sum_{i=m+2}^L \boldsymbol{\Omega}(L, i) \mathbf{W}^{(i)} \underline{\mathbf{b}}^{(i-1)} + \boldsymbol{\Omega}(L, m) \mathbf{b}^{(m)} + \boldsymbol{\Omega}(L, m+1) \mathbf{W}^{(m+1)} \underline{\mathbf{b}}^{(m)} \\
&= \sum_{i=m}^L \boldsymbol{\Omega}(L, i) \mathbf{b}^{(i)} + \sum_{i=m+1}^L \boldsymbol{\Omega}(L, i) \mathbf{W}^{(i)} \underline{\mathbf{b}}^{(i-1)} \\
&= c^{(m-1)}
\end{aligned}$$

For  $\mathbf{P}' := [\mathbf{P}'_m^\top \cdots \mathbf{P}'_{L-1}^\top]$ , we have a new block  $\mathbf{P}'_m$  where

$$\mathbf{P}'_m = \mathbf{S}^{(m)} \mathbf{W}^{(m)} = \mathbf{S}^{(m)} \boldsymbol{\Omega}(m, m) \mathbf{W}^{(m)} = \mathbf{P}_m^{(m-1)}$$

for other blocks where  $m+1 \leq i \leq L-1$ ,

$$\mathbf{P}'_i = \mathbf{P}_i^{(m)} \mathbf{D}^{(m)} \mathbf{W}^{(m)} = \mathbf{S}^{(i)} \boldsymbol{\Omega}(i, m+1) \mathbf{W}^{(m+1)} \mathbf{D}^{(m)} \mathbf{W}^{(m)} = \mathbf{S}^{(i)} \boldsymbol{\Omega}(i, m) \mathbf{W}^{(m)} = \mathbf{P}_i^{(m-1)}$$

For  $\mathbf{q}' := [\mathbf{q}'_m^\top \cdots \mathbf{q}'_{L-1}^\top]$ , we have a new block  $\mathbf{q}'_m$  where

$$\mathbf{q}'_m = \mathbf{S}^{(m)} \mathbf{b}^{(m)} = \sum_{k=m}^m \mathbf{S}^{(i)} \boldsymbol{\Omega}(i, k) \mathbf{b}^{(i)} = \mathbf{q}_m^{(m-1)}$$

for other blocks where  $m+1 \leq i \leq L-1$ ,

$$\begin{aligned}
\mathbf{q}'_i &= \mathbf{q}_i^{(m)} + \mathbf{P}^{(m)\top} \mathbf{D}^{(m)} \mathbf{b}^{(m)} + \mathbf{P}^{(m)\top} \underline{\mathbf{b}}^{(m)} \\
&= \sum_{k=m+1}^i \mathbf{S}^{(i)} \boldsymbol{\Omega}(i, k) \mathbf{b}^{(k)} + \sum_{k=m+2}^i \mathbf{S}^{(i)} \boldsymbol{\Omega}(i, k) \mathbf{W}^{(k)} \underline{\mathbf{b}}^{(k-1)} + \mathbf{P}^{(m)\top} \mathbf{D}^{(m)} \mathbf{b}^{(m)} + \mathbf{P}^{(m)\top} \underline{\mathbf{b}}^{(m)} \\
&= \sum_{k=m+1}^i \mathbf{S}^{(i)} \boldsymbol{\Omega}(i, k) \mathbf{b}^{(k)} + \sum_{k=m+2}^i \mathbf{S}^{(i)} \boldsymbol{\Omega}(i, k) \mathbf{W}^{(k)} \underline{\mathbf{b}}^{(k-1)} + \mathbf{S}^{(i)} \boldsymbol{\Omega}(i, m+1) \mathbf{W}^{(m+1)} \mathbf{D}^{(m)} \mathbf{b}^{(m)} + \mathbf{S}^{(i)} \boldsymbol{\Omega}(i, m+1) \mathbf{W}^{(m+1)} \underline{\mathbf{b}}^{(k)} \\
&= \sum_{k=m+1}^i \mathbf{S}^{(i)} \boldsymbol{\Omega}(i, k) \mathbf{b}^{(k)} + \sum_{k=m+2}^i \mathbf{S}^{(i)} \boldsymbol{\Omega}(i, k) \mathbf{W}^{(k)} \underline{\mathbf{b}}^{(k-1)} + \mathbf{S}^{(i)} \boldsymbol{\Omega}(i, m) \mathbf{b}^{(m)} + \mathbf{S}^{(i)} \boldsymbol{\Omega}(i, m+1) \mathbf{W}^{(m+1)} \underline{\mathbf{b}}^{(m)} \\
&= \sum_{k=m}^i \mathbf{S}^{(i)} \boldsymbol{\Omega}(i, k) \mathbf{b}^{(k)} + \sum_{k=m+1}^i \mathbf{S}^{(i)} \boldsymbol{\Omega}(i, k) \mathbf{W}^{(k)} \underline{\mathbf{b}}^{(k-1)} \\
&= \mathbf{q}_i^{(m-1)}
\end{aligned}$$

Thus,  $\mathbf{a}' = \mathbf{a}^{(m-1)}$ ,  $\mathbf{P}' = \mathbf{P}^{(m-1)}$ ,  $\mathbf{q}' = \mathbf{q}^{(m-1)}$  and  $c' = c^{(m-1)}$  so the induction holds for layer  $\hat{z}^{(m-1)}$ :

$$\min_{\substack{x \in \mathcal{C} \\ z \in \mathcal{Z}}} f(x) \geq \max_{\tilde{\boldsymbol{\beta}}^{(m)} \geq 0} \min_{\substack{x \in \mathcal{C} \\ \hat{z}^{(m-1)} \in \hat{\mathcal{Z}}^{(m-1)}}} (\mathbf{a}^{(m-1)} + \mathbf{P}^{(m-1)} \tilde{\boldsymbol{\beta}}^{(m)})^\top \hat{z}^{(m-1)} + \mathbf{q}^{(m-1)\top} \tilde{\boldsymbol{\beta}}^{(m)} + c^{(m-1)} \quad (27)$$

Finally, Theorem 3.1 becomes the special case where  $m=0$  in Eq. 21, Eq. 22, Eq. 23 and Eq. 24.  $\square$

The next Lemma unveils the connection with CROWN (Zhang et al., 2018) and is also useful for drawing connections to the dual problem.

**Lemma A.2.** *With  $\mathbf{D}$ ,  $\underline{\mathbf{b}}$  and  $\mathbf{A}$  defined in Eq. 18, Eq. 19 and Eq. 20, we can rewrite Eq. 13 in Theorem 3.1 as:*

$$\min_{\substack{x \in \mathcal{C} \\ z \in \mathcal{Z}}} f(x) \geq \max_{\boldsymbol{\beta} \geq 0} \min_{x \in \mathcal{C}} \mathbf{A}^{(0)} x + \sum_{i=1}^{L-1} \mathbf{A}^{(i)} (\mathbf{D}^{(i)} \mathbf{b}^{(i)} + \underline{\mathbf{b}}^{(i)}) \quad (28)$$

where  $\mathbf{A}^{(i)}$ ,  $0 \leq i \leq L-1$  contains variables  $\boldsymbol{\beta}$ .

*Proof.* To prove this lemma, we simply follow the definition of  $\mathbf{A}^{(i)}$  and check the resulting terms are the same as Eq. 13. For example,

$$\begin{aligned}
\mathbf{A}^{(0)} &= (\mathbf{A}^{(1)} \mathbf{D}^{(1)} + \boldsymbol{\beta}^{(1)\top} \mathbf{S}^{(1)}) \mathbf{W}^{(1)} \\
&= \mathbf{A}^{(1)} \mathbf{D}^{(1)} \mathbf{W}^{(1)} + \boldsymbol{\beta}^{(1)\top} \mathbf{S}^{(1)} \mathbf{W}^{(1)} \\
&= (\mathbf{A}^{(2)} \mathbf{D}^{(2)} + \boldsymbol{\beta}^{(2)\top} \mathbf{S}^{(2)}) \mathbf{W}^{(2)} \mathbf{D}^{(1)} \mathbf{W}^{(1)} + \boldsymbol{\beta}^{(1)\top} \mathbf{S}^{(1)} \mathbf{W}^{(1)} \\
&= \mathbf{A}^{(2)} \mathbf{D}^{(2)} \mathbf{W}^{(2)} \mathbf{D}^{(1)} \mathbf{W}^{(1)} + \boldsymbol{\beta}^{(2)\top} \mathbf{S}^{(2)} \mathbf{W}^{(2)} \mathbf{D}^{(1)} \mathbf{W}^{(1)} + \boldsymbol{\beta}^{(1)\top} \mathbf{S}^{(1)} \mathbf{W}^{(1)} \\
&= \dots \\
&= \boldsymbol{\Omega}(L, 1) \mathbf{W}^{(1)} + \sum_{i=1}^{L-1} \boldsymbol{\beta}^{(i)\top} \mathbf{S}^{(i)} \boldsymbol{\Omega}(i, 1) \mathbf{W}^{(1)} \\
&= [\mathbf{a} + \mathbf{P}\boldsymbol{\beta}]^\top
\end{aligned}$$

Other terms can be shown similarly.  $\square$

With this definition of  $\mathbf{A}$ , we can see Eq. 13 as a modified form of CROWN, with an extra term  $\boldsymbol{\beta}^{(i+1)\top} \mathbf{S}^{(i+1)}$  added when computing  $\mathbf{A}^{(i)}$ . When we set  $\boldsymbol{\beta} = 0$ , we obtain the same bound propagation rule for  $\mathbf{A}$  as in CROWN. Thus, only a small change is needed to implement  $\beta$ -CROWN given an existing CROWN implementation: we add  $\boldsymbol{\beta}^{(i+1)\top} \mathbf{S}^{(i+1)}$  after the linear bound propagates backwards through a ReLU layer. We also have the same observation in the dual space, as we will show this connection in the next subsection.

## A.2. Proofs for the connection to the dual space

**Theorem 3.2.** *The objective  $d_{LP}$  for the dual problem of Eq. 8 can be represented as*

$$d_{LP} = -\|\mathbf{a} + \mathbf{P}\boldsymbol{\beta}\|_1 \cdot \epsilon + (\mathbf{P}^\top \mathbf{x}_0 + \mathbf{q})^\top \boldsymbol{\beta} + \mathbf{a}^\top \mathbf{x}_0 + c,$$

where  $\mathbf{a}$ ,  $\mathbf{P}$ ,  $\mathbf{q}$  and  $c$  are defined in the same way as in Theorem 3.1, and  $\boldsymbol{\beta} \geq 0$  corresponds to the dual variables of neuron split constraints in Eq. 8.

*Proof.* To prove the Theorem 3.2, we demonstrate the detailed dual objective  $d_{LP}$  for Eq. 8, following a construction similar to the one in Wong & Kolter (2018). We first associate a dual variable for each constraint involved in Eq. 8 including dual variables  $\boldsymbol{\beta}$  for the per-neuron split constraints introduced by BaB. Although it is possible to directly write the dual LP for Eq. 8, for easier understanding, we first rewrite the original primal verification problem into its Lagrangian dual form as Eq. 29, with dual variables  $\boldsymbol{\nu}$ ,  $\boldsymbol{\xi}$ ,  $\boldsymbol{\mu}$ ,  $\boldsymbol{\gamma}$ ,  $\boldsymbol{\lambda}$ ,  $\boldsymbol{\beta}$ :

$$\begin{aligned}
L(z, \hat{z}; \boldsymbol{\nu}, \boldsymbol{\xi}, \boldsymbol{\mu}, \boldsymbol{\gamma}, \boldsymbol{\lambda}, \boldsymbol{\beta}) &= z^{(L)} + \sum_{i=1}^L \boldsymbol{\nu}^{(i)\top} (z^i - \mathbf{W}^{(i)} \hat{z}^{i-1} - \mathbf{b}^{(i)}) \\
&\quad + \boldsymbol{\xi}^{+\top} (\hat{z}^{(0)} - \mathbf{x}_0 - \epsilon) + \boldsymbol{\xi}^{-\top} (-\hat{z}^{(0)} + \mathbf{x}_0 - \epsilon) \\
&\quad + \sum_{i=1}^{L-1} \sum_{\substack{j \notin \mathcal{Z}^{+(i)} \cup \mathcal{Z}^{-(i)} \\ \mathbf{l}_j^{(i)} < 0 < \mathbf{u}_j^{(i)}}} \left[ \boldsymbol{\mu}_j^{(i)\top} (-\hat{z}_j^{(i)}) + \boldsymbol{\gamma}_j^{(i)\top} (z_j^{(i)} - \hat{z}_j^{(i)}) + \boldsymbol{\lambda}_j^{(i)\top} (-\mathbf{u}_j^{(i)} z_j^{(i)} + (\mathbf{u}_j^{(i)} - \mathbf{l}_j^{(i)}) \hat{z}_j^{(i)} + \mathbf{u}_j^{(i)} \mathbf{l}_j^{(i)}) \right] \\
&\quad + \sum_{i=1}^{L-1} \left[ \sum_{z_j^{(i)} \in \mathcal{Z}^{-(i)}} \boldsymbol{\beta}_j^{(i)} z_j^{(i)} + \sum_{z_j^{(i)} \in \mathcal{Z}^{+(i)}} -\boldsymbol{\beta}_j^{(i)} z_j^{(i)} \right]
\end{aligned} \tag{29}$$

Subject to:

$$\boldsymbol{\xi}, \boldsymbol{\mu}, \boldsymbol{\gamma}, \boldsymbol{\lambda}, \boldsymbol{\beta} \geq 0$$

The original minimization problem then becomes:

$$\max_{\boldsymbol{\nu}, \boldsymbol{\xi}, \boldsymbol{\mu}, \boldsymbol{\gamma}, \boldsymbol{\lambda}, \boldsymbol{\beta}} \min_{z, \hat{z}} L(z, \hat{z}, \boldsymbol{\nu}, \boldsymbol{\xi}, \boldsymbol{\mu}, \boldsymbol{\gamma}, \boldsymbol{\lambda}, \boldsymbol{\beta})$$

Given fixed intermediate bounds  $\mathbf{l}, \mathbf{u}$ , the inner minimization is a linear optimization problem and we can simply transfer it to the dual form. To further simplify the formula, we introduce notations similar to those in (Wong & Kolter, 2018), where  $\hat{\boldsymbol{\nu}}^{(i-1)} = \mathbf{W}^{(i)\top} \boldsymbol{\nu}^{(i)}$  and  $\boldsymbol{\alpha}_j^{(i)} = \frac{\boldsymbol{\gamma}_j^{(i)}}{\boldsymbol{\mu}_j^{(i)} + \boldsymbol{\gamma}_j^{(i)}}$ . Then the dual form can be written as Eq. 30.

$\max_{0 \leq \boldsymbol{\alpha} \leq 1, \boldsymbol{\beta} \geq 0} g(\boldsymbol{\alpha}, \boldsymbol{\beta})$ , where

$$g(\boldsymbol{\alpha}, \boldsymbol{\beta}) = -\sum_{i=1}^L \boldsymbol{\nu}^{(i)\top} \mathbf{b}^{(i)} - \hat{\boldsymbol{\nu}}^{(0)\top} x_0 - \|\hat{\boldsymbol{\nu}}^{(0)}\|_1 \cdot \epsilon + \sum_{i=1}^{L-1} \sum_{\substack{j \notin \mathcal{Z}^{+(i)} \cup \mathcal{Z}^{-(i)} \\ \mathbf{l}_j^{(i)} < 0 < \mathbf{u}_j^{(i)}}} \mathbf{l}_j^{(i)} [\boldsymbol{\nu}_j^{(i)}]^+$$

Subject to:

$$\begin{aligned} \boldsymbol{\nu}^{(L)} &= -1, \hat{\boldsymbol{\nu}}^{(i-1)} = \mathbf{W}^{(i)\top} \boldsymbol{\nu}^{(i)}, \quad i \in \{1, \dots, L\} \\ \boldsymbol{\nu}_j^{(i)} &= 0, \quad \text{when } \mathbf{u}_j^{(i)} \leq 0, i \in \{1, \dots, L-1\} \\ \boldsymbol{\nu}_j^{(i)} &= \hat{\boldsymbol{\nu}}_j^{(i)}, \quad \text{when } \mathbf{l}_j^{(i)} \geq 0, i \in \{1, \dots, L-1\} \\ [\boldsymbol{\nu}_j^{(i)}]^+ &= \frac{\mathbf{u}_j^{(i)} [\hat{\boldsymbol{\nu}}_j^{(i)}]^+}{\mathbf{u}_j^{(i)} - \mathbf{l}_j^{(i)}}, [\boldsymbol{\nu}_j^{(i)}]^- = \boldsymbol{\alpha}_j^{(i)} [\hat{\boldsymbol{\nu}}_j^{(i)}]^- \\ \boldsymbol{\lambda}_j^{(i)} &= \frac{[\hat{\boldsymbol{\nu}}_j^{(i)}]^+}{\mathbf{u}_j^{(i)} - \mathbf{l}_j^{(i)}}, \boldsymbol{\alpha}_j^{(i)} = \frac{\boldsymbol{\gamma}_j^{(i)}}{\boldsymbol{\mu}_j^{(i)} + \boldsymbol{\gamma}_j^{(i)}} \quad \left. \right\} \text{when } \mathbf{l}_j^{(i)} < 0 < \mathbf{u}_j^{(i)}, j \notin \mathcal{Z}^{+(i)} \cup \mathcal{Z}^{-(i)}, i \in \{1, \dots, L-1\} \\ \boldsymbol{\nu}_j^{(i)} &= -\boldsymbol{\beta}_j^{(i)}, \quad j \in \mathcal{Z}^{-(i)}, i \in \{1, \dots, L-1\} \\ \boldsymbol{\nu}_j^{(i)} &= \boldsymbol{\beta}_j^{(i)} + \hat{\boldsymbol{\nu}}_j^{(i)}, \quad j \in \mathcal{Z}^{+(i)}, i \in \{1, \dots, L-1\} \\ \boldsymbol{\xi}, \boldsymbol{\mu}, \boldsymbol{\gamma}, \boldsymbol{\lambda}, \boldsymbol{\beta} &\geq 0, 0 \leq \boldsymbol{\alpha} \leq 1 \end{aligned} \tag{30}$$

Similar to the dual form in (Wong & Kolter, 2018) (our differences are highlighted in blue), the dual problem can be viewed in the form of another deep network by backward propagating  $\boldsymbol{\nu}^{(L)}$  to  $\hat{\boldsymbol{\nu}}^{(0)}$  following the rules in Eq. 30. If we look closely at the conditions and coefficients when backward propagating  $\boldsymbol{\nu}_j^{(i)}$  for  $j$ -th ReLU at layer  $i$  in Eq. 30, we can observe that they match exactly to the propagation of diagonal matrices  $\mathbf{D}^{(i)}$ ,  $\mathbf{S}^{(i)}$ , and vector  $\mathbf{b}^{(i)}$  defined in Eq. 18 and Eq. 19. Therefore, using notations in Eq. 18 and Eq. 19 we can essentially simplify the dual LP problem in Eq. 30 to:

$$\begin{aligned} \boldsymbol{\nu}^{(L)} &= -1, \hat{\boldsymbol{\nu}}^{(i-1)} = \mathbf{W}^{(i)\top} \boldsymbol{\nu}^{(i)}, \boldsymbol{\nu}^{(i)} = \mathbf{D}^{(i)} \hat{\boldsymbol{\nu}}^{(i)} - \boldsymbol{\beta}^{(i)} \mathbf{S}^{(i)}, i \in \{L, \dots, 1\} \\ \sum_{\substack{\mathbf{l}_j^{(i)} < 0 < \mathbf{u}_j^{(i)} \\ j \notin \mathcal{Z}^{+(i)} \cup \mathcal{Z}^{-(i)}}} \mathbf{l}_j^{(i)} [\boldsymbol{\nu}_j^{(i)}]^+ &= -\hat{\boldsymbol{\nu}}^{(i)\top} \underline{\mathbf{b}}^{(i)}, j \in \{1, \dots, d_i\}, i \in \{L-1, \dots, 1\} \end{aligned} \tag{31}$$

Then we prove the key claim for this proof with induction where  $\mathbf{a}^{(m)}$  and  $\mathbf{P}^{(m)}$  are defined in Eq. 21 and Eq. 22:

$$\hat{\boldsymbol{\nu}}^{(m)} = -\mathbf{a}^{(m)} - \mathbf{P}^{(m)} \tilde{\boldsymbol{\beta}}^{(m+1)} \tag{32}$$

When  $m = L-1$ , we can have  $\hat{\boldsymbol{\nu}}^{(L-1)} = -\mathbf{a}^{(L-1)} - \mathbf{P}^{(L-1)} \tilde{\boldsymbol{\beta}}^{(L)} = -[\boldsymbol{\Omega}(L, L) \mathbf{W}^{(L)}]^\top - \mathbf{0} = -\mathbf{W}^{(L)\top}$  which is true according to Eq. 31.

Now we assume that  $\hat{\boldsymbol{\nu}}^{(m)} = -\mathbf{a}^{(m)} - \mathbf{P}^{(m)} \tilde{\boldsymbol{\beta}}^{(m+1)}$  holds, and we show that  $\hat{\boldsymbol{\nu}}^{(m-1)} = -\mathbf{a}^{(m-1)} - \mathbf{P}^{(m-1)} \tilde{\boldsymbol{\beta}}^{(m)}$  will

hold as well:

$$\begin{aligned}
\hat{\boldsymbol{\nu}}^{(m-1)} &= \mathbf{W}^{(m)\top} \left( \mathbf{D}^{(m)} \hat{\boldsymbol{\nu}}^{(m)} - \boldsymbol{\beta}^{(m)} \mathbf{S}^{(m)} \right) \\
&= -\mathbf{W}^{(m)\top} \mathbf{D}^{(m)} \mathbf{a}^{(m)} - \mathbf{W}^{(m)\top} \mathbf{D}^{(m)} \mathbf{P}^{(m)} \tilde{\boldsymbol{\beta}}^{(m+1)} - \mathbf{W}^{(m)\top} \boldsymbol{\beta}^{(m)} \mathbf{S}^{(m)} \\
&= -\mathbf{a}^{(m-1)} - \left[ \left( \mathbf{S}^{(m)} \mathbf{W}^{(m)} \right)^\top, \left( \mathbf{P}^{(m)\top} \mathbf{D}^{(m)} \mathbf{W}^{(m)} \right)^\top \right] \left[ \boldsymbol{\beta}^{(m)}, \tilde{\boldsymbol{\beta}}^{(m+1)} \right] \\
&= -\mathbf{a}^{(m-1)} - \mathbf{P}^{(m-1)} \tilde{\boldsymbol{\beta}}^{(m)}
\end{aligned}$$

Therefore, the claim Eq. 32 is proved with induction. Lastly, we prove the following claim where  $\mathbf{q}^{(m)}$  and  $c^{(m)}$  are defined in Eq. 23 and Eq. 24.

$$-\sum_{i=m+1}^L \boldsymbol{\nu}^{(i)\top} \mathbf{b}^{(i)} + \sum_{i=m+1}^{L-1} \sum_{\substack{1_j^{(i)} < 0 < \mathbf{u}_j^{(i)} \\ j \notin \mathcal{Z}^{+(i)} \cup \mathcal{Z}^{-(i)}}} \mathbf{l}_j^{(i)} [\boldsymbol{\nu}_j^{(i)}]^+ = \mathbf{q}^{(m)\top} \tilde{\boldsymbol{\beta}}^{(m+1)} + c^{(m)} \quad (33)$$

This claim can be proved by applying Eq. 31 and Eq. 32.

$$\begin{aligned}
-\sum_{i=m+1}^L \boldsymbol{\nu}^{(i)\top} \mathbf{b}^{(i)} + \sum_{i=m+1}^{L-1} \sum_{\substack{1_j^{(i)} < 0 < \mathbf{u}_j^{(i)} \\ j \notin \mathcal{Z}^{+(i)} \cup \mathcal{Z}^{-(i)}}} \mathbf{l}_j^{(i)} [\boldsymbol{\nu}_j^{(i)}]^+ &= -\sum_{i=m+1}^L \left( \mathbf{D}^{(i)} \hat{\boldsymbol{\nu}}^{(i)} - \boldsymbol{\beta}^{(i)} \mathbf{S}^{(i)} \right)^\top \mathbf{b}^{(i)} + \sum_{i=m+2}^L \left( -\hat{\boldsymbol{\nu}}^{(i-1)\top} \underline{\mathbf{b}}^{(i-1)} \right) \\
&= \sum_{i=m+1}^L \left[ \left( \mathbf{a}^{(i)\top} + \tilde{\boldsymbol{\beta}}^{(i+1)\top} \mathbf{P}^{(i)\top} \right) \mathbf{D}^{(i)} \mathbf{b}^{(i)} + \boldsymbol{\beta}^{(i)\top} \mathbf{S}^{(i)} \mathbf{b}^{(i)} \right] + \sum_{i=m+2}^L \left( \mathbf{a}^{(i-1)\top} + \tilde{\boldsymbol{\beta}}^{(i)\top} \mathbf{P}^{(i-1)\top} \right) \underline{\mathbf{b}}^{(i-1)} \\
&= \sum_{i=m+1}^L \tilde{\boldsymbol{\beta}}^{(i)\top} \left[ \mathbf{S}^{(i)}, \mathbf{P}^{(i)\top} \mathbf{D}^{(i)} \right] \mathbf{b}^{(i)} + \sum_{i=m+2}^L \tilde{\boldsymbol{\beta}}^{(i)\top} \mathbf{P}^{(i-1)\top} \underline{\mathbf{b}}^{(i-1)} + \sum_{i=m+1}^L \mathbf{a}^{(i)\top} \mathbf{D}^{(i)} \mathbf{b}^{(i)} + \sum_{i=m+2}^L \mathbf{a}^{(i-1)\top} \underline{\mathbf{b}}^{(i-1)} \\
&= \mathbf{q}^{(m)\top} \tilde{\boldsymbol{\beta}}^{(m+1)} + c^{(m)}
\end{aligned}$$

Finally, we apply claims Eq. 32 and Eq. 33 into the dual form solution Eq. 30 and prove the Theorem 3.2.

$$\begin{aligned}
g(\boldsymbol{\alpha}, \boldsymbol{\beta}) &= -\sum_{i=1}^L \boldsymbol{\nu}^{(i)\top} \mathbf{b}^{(i)} - \hat{\boldsymbol{\nu}}^{(0)\top} x_0 - \|\hat{\boldsymbol{\nu}}^{(0)}\|_1 \cdot \epsilon + \sum_{i=1}^{L-1} \sum_{\substack{1_j^{(i)} < 0 < \mathbf{u}_j^{(i)} \\ j \notin \mathcal{Z}^{+(i)} \cup \mathcal{Z}^{-(i)}}} \mathbf{l}_j^{(i)} [\boldsymbol{\nu}_j^{(i)}]^+ \\
&= -\|-\mathbf{a}^{(0)} - \mathbf{P}^{(0)} \tilde{\boldsymbol{\beta}}^{(1)}\|_1 \cdot \epsilon + \left( \mathbf{a}^{(0)\top} + \tilde{\boldsymbol{\beta}}^{(1)\top} \mathbf{P}^{(0)\top} \right) x_0 + \mathbf{q}^{(0)\top} \tilde{\boldsymbol{\beta}}^{(1)} + c^{(0)} \\
&= -\|\mathbf{a} + \mathbf{P} \tilde{\boldsymbol{\beta}}^{(1)}\|_1 \cdot \epsilon + (\mathbf{P}^\top x_0 + \mathbf{q})^\top \tilde{\boldsymbol{\beta}}^{(1)} + \mathbf{a}^\top x_0 + c
\end{aligned}$$

**A more intuitive proof.** Here we provide another intuitive proof showing why the dual form solution of verification objective in Eq. 30 is the same as the primal one in Thereom 3.1.  $d_{\text{LP}} = g(\boldsymbol{\alpha}, \boldsymbol{\beta})$  is the dual objective for Eq. 8 with free variables  $\boldsymbol{\alpha}$  and  $\boldsymbol{\beta}$ . We want to show that the dual problem can be viewed in the form of backward propagating  $\boldsymbol{\nu}^{(L)}$  to  $\hat{\boldsymbol{\nu}}^{(0)}$  following the same rules in  $\beta$ -CROWN. Salman et al. (2019) showed that CROWN computes the same solution as the dual form in Wong & Kolter (2018):  $\hat{\boldsymbol{\nu}}^{(i)}$  is corresponding to  $-\mathbf{A}^{(i)}$  in CROWN (defined in the same way as in Eq. 20 but with  $\boldsymbol{\beta}^{(i+1)} = 0$ ) and  $\boldsymbol{\nu}^{(i)}$  is corresponding to  $-\mathbf{A}^{(i+1)} \mathbf{D}^{(i+1)}$ . When the split constraints are introduced, extra terms for the dual variable  $\boldsymbol{\beta}$  modify  $\boldsymbol{\nu}^{(i)}$  (highlighted in blue in Eq. 30). The way  $\beta$ -CROWN modifies  $\mathbf{A}^{(i+1)} \mathbf{D}^{(i+1)}$  is exactly the same as the way  $\boldsymbol{\beta}^{(i)}$  affects  $\boldsymbol{\nu}^{(i)}$ : when we split  $z_j^{(i)} \geq 0$ , we add  $\boldsymbol{\beta}_j^{(i)}$  to the  $\boldsymbol{\nu}_j^{(i)}$  in Wong & Kolter (2018); when we split  $z_j^{(i)} \geq 0$ , we add  $-\boldsymbol{\beta}_j^{(i)}$  to the  $\boldsymbol{\nu}_j^{(i)}$  in Wong & Kolter (2018) ( $\boldsymbol{\nu}_j^{(i)}$  is 0 in this case because it is set to be inactive). To make this relationship more clear, we define a new variable  $\boldsymbol{\nu}'$ , and rewrite relevant terms involving  $\boldsymbol{\nu}$ ,  $\hat{\boldsymbol{\nu}}$  below:

$$\begin{aligned}
\nu_j^{(i)} &= 0, \quad j \in \mathcal{Z}^{-(i)}; \\
\nu_j^{(i)} &= \hat{\nu}_j^{(i)}, \quad j \in \mathcal{Z}^{+(i)}; \\
\nu_j^{(i)} &\text{ is defined in the same way as in Eq. 30 for other cases} \\
\nu_j^{(i)\prime} &= -\beta_j^{(i)} + \nu_j^{(i)}, \quad j \in \mathcal{Z}^{-(i)}; \\
\nu_j^{(i)\prime} &= \beta_j^{(i)} + \nu_j^{(i)}, \quad j \in \mathcal{Z}^{+(i)}; \\
\nu_j^{(i)\prime} &= \nu_j^{(i)}, \quad \text{otherwise} \\
\hat{\nu}^{(i-1)} &= \mathbf{W}^{(i)\top} \nu^{(i)\prime}; 
\end{aligned} \tag{34}$$

It is clear that  $\nu'$  corresponds to the term  $-(\mathbf{A}^{(i+1)} \mathbf{D}^{(i+1)} + \beta^{(i+1)\top} \mathbf{S}^{(i+1)})$  in Eq. 20, by noting that  $\nu^{(i)}$  in (Wong & Kolter, 2018) is equivalent to  $-\mathbf{A}^{(i+1)} \mathbf{D}^{(i+1)}$  in CROWN and the choice of signs in  $\mathbf{S}^{(i+1)}$  reflects neuron split constraints. Thus, the dual formulation will produce the same results as Eq. 28, and thus also equivalent to Eq. 13.  $\square$

**Corollary 3.2.1.** *When  $\alpha$  and  $\beta$  are optimally set,  $\beta$ -CROWN produces the same solution as LP with split constraints when intermediate bounds  $\mathbf{l}, \mathbf{u}$  are fixed. Formally,*

$$\max_{0 \leq \alpha \leq 1, \beta \geq 0} g(\alpha, \beta) = p_{LP}^*$$

where  $p_{LP}^*$  is the optimal objective of Eq. 8.

*Proof.* Given fixed intermediate layer bounds  $\mathbf{l}$  and  $\mathbf{u}$ , the dual form of the verification problem in Eq. 8 is a linear programming problem with dual variables defined in Eq. 29. Suppose we use an LP solver to obtain the optimal dual solution  $\nu^*, \xi^*, \mu^*, \gamma^*, \lambda^*, \beta^*$ . Then we can set  $\alpha_j^{(i)} = \frac{\gamma_j^{(i)*}}{\mu_j^{(i)*} + \gamma_j^{(i)*}}$ ,  $\beta = \beta^*$  and plug them into Eq. 30 to get the optimal dual solution  $d_{LP}^*$ . Theorem 3.2 shows that,  $\beta$ -CROWN can compute the same objective  $d_{LP}^*$  given the same  $\alpha_j^{(i)} = \frac{\gamma_j^{(i)*}}{\mu_j^{(i)*} + \gamma_j^{(i)*}}$ ,  $\beta = \beta^*$ , thus  $\max_{0 \leq \alpha \leq 1, \beta \geq 0} g(\alpha, \beta) \geq d_{LP}^*$ . On the other hand, for any setting of  $\alpha$  and  $\beta$ ,  $\beta$ -CROWN produces the same solution  $g(\alpha, \beta)$  as the rewritten dual LP in Eq. 30, so  $g(\alpha, \beta) \leq d_{LP}^*$ . Thus, we have  $\max_{0 \leq \alpha \leq 1, \beta \geq 0} g(\alpha, \beta) = d_{LP}^*$ . Finally, due to the strong duality in linear programming,  $p_{LP}^* = d_{LP}^* = \max_{0 \leq \alpha \leq 1, \beta \geq 0} g(\alpha, \beta)$ .  $\square$

The variables  $\alpha$  in  $\beta$ -CROWN can be translated to dual variables in LP as well. Given  $\alpha^*$  in  $\beta$ -CROWN, we can get the corresponding dual LP variables  $\mu, \gamma$  given  $\alpha$  by setting  $\mu_j^{(i)} = (1 - \alpha_j^{(i)})[\hat{\nu}_j^{(i)}]^-$  and  $\gamma_j^{(i)} = \alpha_j^{(i)}[\hat{\nu}_j^{(i)}]^-$ .

### A.3. Proof for soundness and completeness

**Theorem 3.3.**  *$\beta$ -CROWN with branch and bound on splitting ReLU neurons is sound and complete.*

*Proof.* **Soundness.** Branch and bound (BaB) with  $\beta$ -CROWN is sound because for each subdomain  $\mathcal{C}_i := \{x \in \mathcal{C}, z \in \mathcal{Z}_i\}$ , we apply Theorem 3.1 to obtain a sound lower bound  $\underline{f}_{\mathcal{C}_i}$  (the bound is valid for any  $\beta \geq 0$ ). The final bound returned by BaB is  $\min_i \underline{f}_{\mathcal{C}_i}$  which represents the worst case over all subdomains, and is a sound lower bound for  $x \in \mathcal{C} := \bigcup_i \mathcal{C}_i$ .

**Completeness.** To show completeness, we need to solve Eq. 1 to its global minimum. When there are  $N$  unstable neurons, we have up to  $2^N$  subdomains, and in each subdomain we have all unstable ReLU neurons split into one of the  $z_j^{(i)} \geq 0$  or  $z_j^{(i)} < 0$  case. The final solution obtained by BaB is the min over these  $2^N$  subdomains. To obtain the global minimum, we must ensure that in every of these  $2^N$  subdomain we can solve Eq. 8 exactly.

When all unstable neurons are split in a subdomain  $\mathcal{C}_i$ , the network becomes a linear network and neuron split constraints become linear constraints w.r.t. inputs. Under this case, an LP with Eq. 8 can solve the verification problem in  $\mathcal{C}_i$  exactly. In  $\beta$ -CROWN, we solve the subdomain using the usually non-concave formulation Eq. 10; however, in this case, it becomes concave in  $\hat{\beta}$  because no intermediate layer bounds are used (no  $\alpha'$  and  $\beta'$ ) and no ReLU neuron is relaxed (no  $\alpha$ ), thus

---

**Algorithm 1**  $\beta$ -CROWN with branch and bound for complete verification. **Comments** are in brown.

---

```

1: Inputs:  $f, \mathcal{C}, n$  (batch size),  $\delta$  (tolerance),  $\eta$  (maximum length of sub-domains)
2:  $(\underline{f}, \bar{f}) \leftarrow \text{optimized\_beta\_CROWN}(f, [\mathcal{C}])$  ▷ Initially there is no split, so optimization is done over  $\hat{\alpha}$ 
3:  $\mathbb{P} \leftarrow [(\underline{f}, \bar{f}, \mathcal{C})]$  ▷  $\mathbb{P}$  is the set of all unverified sub-domains
4: while  $\underline{f} < 0$  and  $\bar{f} \geq 0$  and  $\bar{f} - \underline{f} > \delta$  and  $\text{length}(\mathbb{P}) < \eta$  do
5:    $(\mathcal{C}_1, \dots, \mathcal{C}_n) \leftarrow \text{batch\_pick\_out}(\mathbb{P}, n)$  ▷ Pick sub-domains to split and removed them from  $\mathbb{P}$ 
6:    $[\mathcal{C}_1^l, \mathcal{C}_1^u, \dots, \mathcal{C}_n^l, \mathcal{C}_n^u] \leftarrow \text{batch\_split}(\mathcal{C}_1, \dots, \mathcal{C}_n)$  ▷ Each  $\mathcal{C}_i$  splits into two sub-domains  $\mathcal{C}_i^l$  and  $\mathcal{C}_i^u$ 
7:    $[\underline{f}_{\mathcal{C}_1^l}, \bar{f}_{\mathcal{C}_1^l}, \underline{f}_{\mathcal{C}_1^u}, \bar{f}_{\mathcal{C}_1^u}, \dots, \underline{f}_{\mathcal{C}_n^l}, \bar{f}_{\mathcal{C}_n^l}, \underline{f}_{\mathcal{C}_n^u}, \bar{f}_{\mathcal{C}_n^u}] \leftarrow \text{optimized\_beta\_CROWN}(f, [\mathcal{C}_1^l, \mathcal{C}_1^u, \dots, \mathcal{C}_n^l, \mathcal{C}_n^u])$  ▷ Compute lower and upper bounds by optimizing  $\hat{\alpha}$  and  $\hat{\beta}$  mentioned in Section 3.3 in a batch
8:    $\mathbb{P} \leftarrow \mathbb{P} \cup \text{Domain\_Filter}([\underline{f}_{\mathcal{C}_1^l}, \bar{f}_{\mathcal{C}_1^l}, \mathcal{C}_1^l], [\underline{f}_{\mathcal{C}_1^u}, \bar{f}_{\mathcal{C}_1^u}, \mathcal{C}_1^u], \dots, [\underline{f}_{\mathcal{C}_n^l}, \bar{f}_{\mathcal{C}_n^l}, \mathcal{C}_n^l], [\underline{f}_{\mathcal{C}_n^u}, \bar{f}_{\mathcal{C}_n^u}, \mathcal{C}_n^u])$  ▷ Filter out verified sub-domains, insert the left domains back to  $\mathbb{P}$ 
9:    $\underline{f} \leftarrow \min\{\underline{f}_{\mathcal{C}_i} \mid (\underline{f}_{\mathcal{C}_i}, \bar{f}_{\mathcal{C}_i}, \mathcal{C}_i) \in \mathbb{P}\}, i = 1, \dots, n$  ▷ To ease notation,  $\mathcal{C}_i$  here indicates either  $\mathcal{C}_i^u$  or  $\mathcal{C}_i^l$ 
10:   $\bar{f} \leftarrow \min\{\bar{f}_{\mathcal{C}_i} \mid (\underline{f}_{\mathcal{C}_i}, \bar{f}_{\mathcal{C}_i}, \mathcal{C}_i) \in \mathbb{P}\}, i = 1, \dots, n$ 
11: Outputs:  $\underline{f}, \bar{f}$ 

```

---

the only optimizable variable is  $\beta$  (Eq. 10 becomes Eq. 6). Eq. 6 is concave in  $\beta$  so (super)gradient ascent guarantees to converge to the global optimal  $\beta^*$ . To ensure convergence without relying on a preset learning rate, a line search can be performed in this case. Then, according to Corollary 3.2.1, this optimal  $\beta^*$  corresponds to the optimal dual variable for the LP in Eq. 8 and the objective is a global minimum of Eq. 8.  $\square$

## B. More details on $\beta$ -CROWN with branch and bound (BaB)

### B.1. $\beta$ -CROWN with branch and bound for complete verification

We list our  $\beta$ -CROWN with branch and bound based complete verifier ( $\beta$ -CROWN BABS) in Algorithm 1. The algorithm takes a target NN function  $f$  and a domain  $\mathcal{C}$  as inputs. The subprocedure `optimized_beta_CROWN` optimizes  $\hat{\alpha}$  and  $\hat{\beta}$  (free variables for computing intermediate layer bounds and last layer bounds) as Eq. 10 in Section 3.3. It operates in a batch and returns the lower and upper bounds for  $n$  selected subdomains simultaneously: a lower bound is obtained by optimizing Eq. 10 using  $\beta$ -CROWN and an upper bound can be the network prediction given the  $x^*$  that minimizes Eq. 5<sup>2</sup>. Initially, we don't have any splits, so we only need to optimize  $\hat{\alpha}$  to obtain  $\underline{f}$  for  $x \in \mathcal{C}$  (Line 2). Then we utilize the power of GPUs to split in parallel and maintain a global set  $\mathbb{P}$  storing all the sub-domains which does not satisfy  $\underline{f}_{\mathcal{C}_i} < 0$  (Line 5-10). Specifically, `batch_pick_out` extends BaBSR (Bunel et al., 2018) in a parallel manner to select  $n$  (batch size) sub-domains in  $\mathbb{P}$  and determine the corresponding ReLU neuron to split for each of them. If the length of  $\mathbb{P}$  is less than  $n$ , then we reduce  $n$  to the length of  $\mathbb{P}$ . `batch_split` splits each selected  $\mathcal{C}_i$  to two sub-domains  $\mathcal{C}_i^l$  and  $\mathcal{C}_i^u$  by forcing the selected unstable ReLU neuron to be positive and negative, respectively. `Domain_Filter` filters out verified sub-domains (proved with  $\underline{f}_{\mathcal{C}_i} \geq 0$ ) and we insert the remaining ones to  $\mathbb{P}$ . The loop breaks if the property is proved ( $\underline{f} \geq 0$ ), or a counter-example is found in any sub-domain ( $\bar{f} < 0$ ), or the lower bound  $\underline{f}$  and upper bound  $\bar{f}$  are sufficiently close, or the length of sub-domains  $\mathbb{P}$  reaches a desired threshold  $\eta$  (maximum memory limit).

### B.2. Comparisons to other GPU based complete verifiers

Bunel et al. (2020a) proposed to reformulate the linear programming problem in Eq. 8 through Lagrangian decomposition. Eq. 8 is decomposed layer by layer, and each layer is solved with simple closed form solutions on GPUs. A Lagrangian is used to enforce the equality between the output of a previous layer and the input of a later layer. This optimization formulation has the same power as a LP (Eq. 8) under convergence. The main drawback of this approach is that it converges relatively slowly (we find that it typically requires hundreds of iterations to converge to a solution similar to the solution of a LP), and it also cannot easily jointly optimize intermediate layer bounds. In Table 2 (PROX BABS) and Figure 2 (BDD+ BABS, which refers to the same method) we can see that this approach is relatively slow and has high timeout rates compared to other GPU accelerated complete verifiers.

<sup>2</sup>We want an upper bound of the objective in Eq. 1. Since Eq. 1 is a minimization problem, any feasible  $x$  produces an upper bound of the optimal objective. When Eq. 1 is solved exactly as  $f^*$  (such as in the case where all neurons are split), we have  $f^* = \underline{f} = \bar{f}$ . See also the discussions in Section I.1 of De Palma et al. (2021).

De Palma et al. (2021) used a tighter convex relaxation (Anderson et al., 2020) than the typical LP formulation in Eq. 8 for the incomplete verifier. This tighter relaxation contains exponentially many constraints, and De Palma et al. (2021) proposed to solve the verification problem in its dual form where each constraint becomes a dual variable. A small active set of dual variables is maintained during dual optimization to ensure efficiency. This tighter relaxation allows it to outperform (Bunel et al., 2020a), but it also comes with extra computational costs and difficulties for an efficient implementation (e.g. a “masked” forward/backward pass is needed which requires a customised lower-level convolution implementation). Additionally, De Palma et al. (2021) did not optimize intermediate layer bounds jointly.

Xu et al. (2021) used CROWN (Zhang et al., 2018) (categorized as a linear relaxation based perturbation analysis (LiRPA) algorithm) as the incomplete solver in BaB. Since CROWN cannot encode neural split constraints, Xu et al. (2021) essentially solve Eq. 8 *without* neuron split constraints ( $z_j^{(i)} \geq 0, i \in \{1, \dots, L-1\}, j \in \mathcal{Z}^{+(i)}$  and  $z_j^{(i)} < 0, i \in \{1, \dots, L-1\}, j \in \mathcal{Z}^{-(i)}$ ) in Eq. 8. The missing constraints lead to looser bounds and more branches - this can be seen in Table 2, where their number of branches and timeout rates are higher than ours. Additionally, using CROWN as the incomplete solver leads to incompleteness - even when all unstable ReLU neurons are split, Xu et al. (2021) still cannot solve Eq. 1 to a global minimum, so a LP solver has to be used to check inconsistent splits and guarantee completeness. Our  $\beta$ -CROWN BaBSR overcomes these drawbacks: we consider per-neuron split constraints in  $\beta$ -CROWN which reduces the number of branches and solving time (Table 2). Most importantly,  $\beta$ -CROWN with branch and bound is sound and complete (Theorem 3.3) and we do not rely on any LP solvers.

Another difference between Xu et al. (2021) and our method is the joint optimization of intermediate layer bounds (Section 3.3). Although (Xu et al., 2021) also optimized intermediate layer bounds, they only optimize  $\alpha$  and do not have  $\beta$ , and they share the same variable  $\alpha$  for all intermediate layer bounds and final bounds, with a total of  $O(Ld)$  variables to optimize. Our analysis in Section 3.3 shows that there are in fact,  $O(L^2d^2)$  free variables to optimize, and we share less variables as in Xu et al. (2021). This allows us to achieve tighter bounds and improve overall performance.

## C. Details on Experimental Setup and Results

### C.1. Experimental Setup

We run our experiments on a single NVIDIA GTX 1080 Ti GPU (11GB memory) and a Intel i7-7700K CPU (4.2 GHz). The memory constraint for all methods is set to 32GB. We use the Adam optimizer (Kingma & Ba, 2014) to solve both  $\hat{\alpha}$  and  $\hat{\beta}$  in Eq. 10 with 20 iterations. The learning rates are set as 0.1 and 0.05 for optimizing  $\hat{\alpha}$  and  $\hat{\beta}$  respectively. We decay the learning rates with a factor of 0.98 per iteration. To maximize the benefits of parallel computing on GPU, we use batch sizes  $n = 200, 128, 400, 200$  and  $200$  for CNN-A-Adv (MNIST), CNN-B-Adv (CIFAR-10), Base (CIFAR-10), Wide (CIFAR-10) and Deep (CIFAR-10) models, respectively. The CNN-A-Adv and CNN-B-Adv models are the same as the models used in (Dathathri et al., 2020). We summarize the model structures in both incomplete verification (CNN-A-Adv and CNN-B-Adv) and complete verification (Base, Wide and Deep) experiments in Table 3.

Table 3. Model structures used in our experiments. For example, Conv(1, 16, 4) stands for a conventional layer with 1 input channel, 16 output channels and a kernel size of  $4 \times 4$ . Liner(1568, 100) stands for a fully connected layer with 1568 input features and 100 output features. We have ReLU activation functions between two consecutive layers.

Model name	Model structure
CNN-A-Adv	Conv(1, 16, 4) - Conv(16, 32, 4) - Linear(1568, 100) - Liner(100, 10)
CNN-B-Adv	Conv(3, 32, 5) - Conv(32, 128, 4) - Linear(8192, 250) - Liner(250, 10)
Base	Conv(3, 8, 4) - Conv(8, 16, 4) - Linear(1024, 100) - Liner(100, 10)
Wide	Conv(3, 16, 4) - Conv(16, 32, 4) - Linear(2048, 100) - Liner(100, 10)
Deep	Conv(3, 8, 4) - Conv(8, 8, 3) - Conv(8, 8, 3) - Conv(8, 8, 4) - Linear(412, 100) - Liner(100, 10)

### C.2. Additional Experiments

**Comparison to LPs with different intermediate layer bounds.** In Figure 3, we compare our  $\beta$ -CROWN BaBSR (3 minutes as the time threshold per verification instance) against incomplete LP verifiers constructed using different intermediate layer bounds obtained from (Wong & Kolter, 2018), CROWN (Zhang et al., 2018), and our joint optimization

Figure 3. Verified lower bound on  $f(x)$  by  $\beta$ -CROWN BaBSR compared against incomplete LP verifiers using different intermediate layer bounds obtained from (Wong & Kolter, 2018) (denoted as LP (WK)), CROWN (Zhang et al., 2018) (denoted as LP (CROWN)), and jointly optimized intermediate bounds in Eq. 10 (denoted as LP (OPT)), v.s. the adversarial upper bound on  $f(x)$  found by PGD.

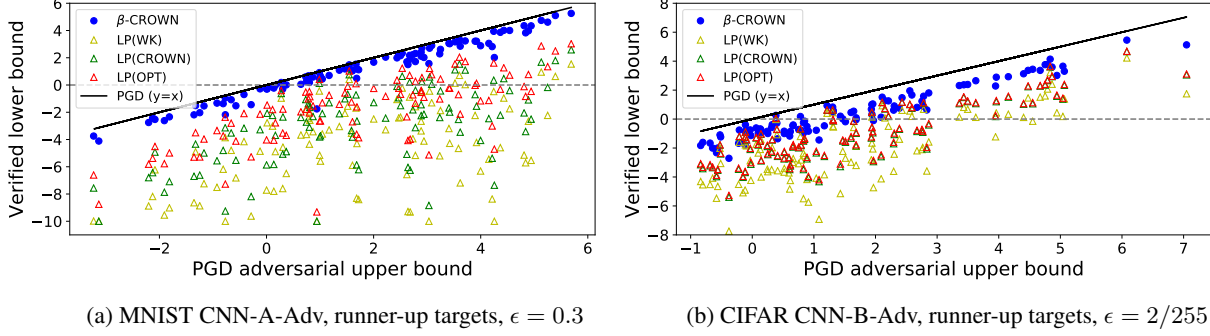
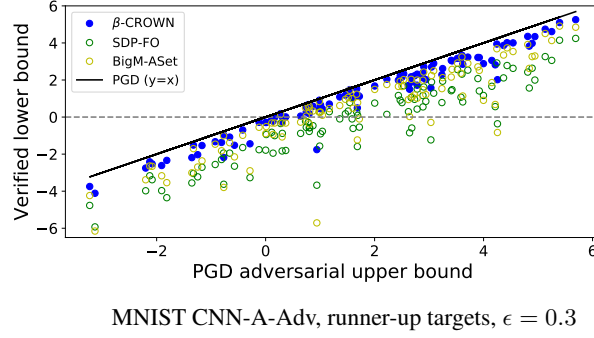


Figure 4. Verified lower bound on  $f(x)$  by  $\beta$ -CROWN BABS and the state-of-the-art complete verifier BIGM+A.SET BABS (which is one of the strongest baselines in Table 2). We set the timeout threshold to 3 minutes per instance for  $\beta$ -CROWN BABS and BIGM+A.SET BABS. We also include SDP-PO and PGD results for reference. SDP-FO takes 2 to 3 hours to converge per instance.



procedure (optimizing Eq. 10 with no  $\hat{\beta}$ ). Our  $\beta$ -CROWN BaBSR always outperforms these three LP verifiers using different intermediate bounds. Also, we show that tighter intermediate layer bounds obtained by CROWN can greatly improve the performance of the LP verifier compared to those using looser ones obtained by (Wong & Kolter, 2018). Furthermore, using intermediate layer bounds computed by our joint optimization can achieve further improvements. The corresponding verified accuracy for each method on PGD trained CNN-A-Adv (MNIST) and CNN-B-Adv (CIFAR-10) networks can be found in Table 4. The results match the observations in Figure 3: tighter intermediate bounds are helpful for LPs, but branch and bound with  $\beta$ -CROWN can significantly outperform these LP verifiers. This shows that BaB is an effective approach for incomplete verification, outperforming the bounds produced by a single LP.

**Comparison to other incomplete verifiers** In addition, we run RefinePoly with k-ReLU relaxation (Singh et al., 2019a). k-ReLU uses relaxations over multiple ReLU neurons, and can overcome the single neuron convex relaxation barrier (Salman et al., 2019) in other LP based verifiers. In Table 4, we found that k-ReLU can outperform LP based verifiers in terms of verified accuracy but requires significantly longer running time. However, the verified accuracy obtained by k-ReLU still has a large gap compared to the verified accuracy of SDP-FO and our  $\beta$ -CROWN BaBSR on both MNIST and CIFAR-10 models.

**More results on incomplete verification using complete verifiers with early stop** In our experiments in Table 2, we noticed that BIGM+A.SET BABS (De Palma et al., 2021) is also very competitive among existing state-of-the-art complete verifiers - it runs fast in many cases with low timeout rates. Therefore, we also evaluate BIGM+A.SET BABS with early stop in 3 minutes for the incomplete verification setting as an extension of Section 4.1. The corresponding verified accuracy for each method are reported in Table 4. In Figure 4, we present the lower bounds obtained by BIGM+A.SET BABS on CNN-Adv-A (MNIST) for the same set of points and target labels as in Figure 1(a). Figure 4 shows that BIGM+A.SET BABS often produces better bounds than SDP-FO, however  $\beta$ -CROWN BABS consistently outperforms BIGM+A.SET BABS under the same 3min timeout.

Table 4. Additional verified accuracy comparisons on 100 random test images.

Dataset Perturbation norm ( $\ell_\infty$ )		MNIST $\epsilon = 0.3$	CIFAR-10 $\epsilon = 2/255$
Model (from <a href="#">Dathathri et al. (2020)</a> )	CNN-A-Adv	CNN-B-Adv	
Number of model parameters	166,406	2,118,856	
Accuracy	Norminal PGD	98.0% 78.0%	78.0% 63.0%
Verified Accuracy	<a href="#">Wong &amp; Kolter (2018)</a> CROWN LP <sup>1</sup> LP (CROWN) <sup>3</sup> LP (OPT) <sup>4</sup> RefinePoly (k-ReLU 15) <sup>6</sup> SDP-FO <sup>2</sup> BigM+A.set BaBSR $\beta$ -CROWN BaBSR	0% 1.0% 1.0% 5.0% 10.0% 15.0% 43.4% 63.0% <b>66.0%</b>	10.0% 22.0% 16.0% 22.0% 22.0% 32.8% N/A <sup>5</sup> <b>35.0%</b>
Avg. Verified Time/Sample	<a href="#">Wong &amp; Kolter (2018)</a> CROWN LP <sup>1</sup> LP (CROWN) <sup>3</sup> LP (OPT) <sup>4</sup> RefinePoly (k-ReLU 15) <sup>6</sup> SDP-FO <sup>2</sup> BigM+A.set BaBSR $\beta$ -CROWN BaBSR	0.02 mins 0.02 mins 3.35 mins 3.34 mins 3.90 mins 22.34 mins 1,274.38 mins 27.00 mins 27.00 mins	0.11 mins 0.11 mins 64.30 mins 64.22 mins 65.25 mins 352.60 mins 1,926.21 mins N/A 27.00 mins

<sup>1</sup> LPs constructed using intermediate bounds from Wong & Kolter.

<sup>2</sup> From 500 test images as reported in [\(Dathathri et al., 2020\)](#).

<sup>3</sup> LPs constructed using intermediate bounds from CROWN.

<sup>4</sup> LPs constructed using jointly optimized intermediate bounds in Eq. 10.

<sup>5</sup> Their code is not compatible with this model with an asymmetric padding layer.

<sup>6</sup> We run RefinePoly with k-ReLU [\(Singh et al., 2019a\)](#), using k=15, LP timeout threshold 10 seconds. Running time is reported using 1 CPU thread.

**Lower bound improvements over time** In Figure 5, we plot lower bound values vs. time for  $\beta$ -CROWN BABSR and BIGM+A.SET BABSR (one of the most competitive methods in Table 2) on the CNN-A-Adv (MNIST) model. Figure 5 shows that branch and bound can indeed quickly improve the lower bound, and our  $\beta$ -CROWN BABSR is consistently faster than BIGM+A.SET BABSR. In contrast, SDP-FO [\(Dathathri et al., 2020\)](#), which typically requires 2 to 3 hours to converge, can only provide very loose bounds during the first 3 minutes of optimization (out of the range on these figures).

**Complete verification performance with averaged metrics** In Section 4 we presented the median of verification time in Table 2. We include mean verification time and number of branches in Table 5. The average verification time is heavily affected by timed out examples. For example, on the Deep model, our  $\beta$ -CROWN with BaBSR significantly outperforms other baselines by over 10X because we have no timeout. This comparison can be misleading because two factors are mixed: the efficiency of the verifier (reflected in verification time for *most* examples) and the capability of the verifier (reflected in the capability of verifying hard examples and producing less timeouts). Instead, median runtime (with timeout rates also in consideration) and the cactus plots in Figure 2 are more appropriate means to gauge the performance of each complete verifier.

Figure 5. For the CNN-A-Adv (MNIST) model, we randomly select four examples from the incomplete verification experiment and plot the lower bound v.s. time (in 180 seconds) of  $\beta$ -CROWN BABS and BIGM+A.SET BABS. Larger lower bounds are better.  $\beta$ -CROWN BABS converges remarkably faster in all four situations.

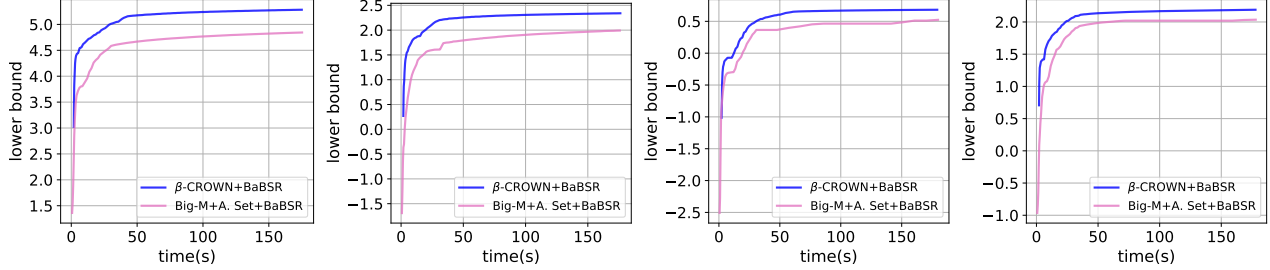


Table 5. Average runtime and average number of branches on three CIFAR-10 models over 100 properties. The average verification time is heavily affected by timed out examples. For example, on the Deep model, our  $\beta$ -CROWN with BABS significantly outperforms other baselines by over 10X because we have no timeout. Instead, median runtime (with timeout rates also in consideration) and the cactus plots in Figure 2 are more appropriate means to gauge the performance of complete verifiers.

Method	Base			Wide			Deep		
	time(s)	branches	%timeout	time(s)	branches	%timeout	time(s)	branches	%timeout
BABS	2367.78	1020.55	36.00	2871.14	812.65	49.00	2750.75	401.28	39.00
MIPPLANET	2849.69	-	68.00	2417.53	-	46.00	2302.25	-	40.00
GNN-ONLINE	1794.85	565.13	33.00	1367.38	372.74	15.00	1055.33	131.85	4.00
BDD+ BABS	807.91	195480.14	20.00	505.65	74203.11	10.00	266.28	12722.74	4.00
A.SET BABS	381.78	12004.60	<b>7.00</b>	<b>165.91</b>	2233.10	<b>3.00</b>	190.28	2491.55	2.00
BIGM+A.SET BABS	390.44	11938.75	<b>7.00</b>	172.65	4050.59	<b>3.00</b>	177.22	3275.25	2.00
FAST-AND-COMPLETE	695.01	119522.65	17.00	495.88	80519.85	9.00	105.64	2455.11	1.00
$\beta$ -CROWN BABS	<b>342.43</b>	90442.05	8.00	170.25	29495.80	<b>3.00</b>	<b>8.79</b>	259.51	<b>0.00</b>